



Torrefaction of woody biomass under an oxidizing atmosphere and its effect on fixed bed gasification

by

Sergio Andrés Ramos Carmona

Submitted in partial fulfilment of the requirements for the degree of
Master of Science in Engineering

Advisor

Juan Fernando Pérez Bayer

University of Antioquia

Medellín

© 2016

All Rights Reserved

Table of Contents

List of Tables	v
List of Figures.....	vi
Acknowledgements	vii
Chapter 1: Study of fixed bed gasification process of torrefied wood biomass under an oxidizing atmosphere.....	1
1.1. Introduction.....	1
1.2. Research objectives.....	2
1.3. Contribution of this dissertation	3
1.4. Authorship of peer review publications.....	4
1.4.1. Journal articles.....	4
1.4.2. International congress.....	4
References	4
Chapter 2: Physicochemical characterization of torrefied wood biomass under an oxidizing atmosphere – Effect of temperature and residence time.....	7
Abstract.....	7
2.1. Introduction.....	7
2.2. Materials and methods	10
2.2.1. Experimental setup	10
2.2.2. Biomass as feedstock.....	11
2.2.3. Experimental plan.....	12
2.2.4. Torrefaction process characterization.....	13
2.2.5. Biomass physicochemical characterization	13
2.3. Results and discussion	15
2.3.1. Torrefaction process characterization.....	15
2.3.2. Physicochemical characterization of torrefied biomass	18

Conclusions	25
Acknowledgements	26
References	26
Chapter 3: Chemical and structural changes in torrefied wood biomass under an oxidizing atmosphere.....	31
Abstract.....	31
3.1. Introduction.....	31
3.2. Materials and methods	33
3.2.1. Materials	33
3.2.2. Experimental setup and torrefaction process.....	33
3.2.3. Proximate and ultimate analyses	34
3.2.4. Analytical techniques	34
3.3. Results and discussion	35
3.3.1. Proximate and ultimate analyses	35
3.3.2. Thermogravimetric analysis	36
3.3.3. Infrared spectroscopy characterization (FTIR).....	40
3.3.4. Brunauer–Emmett–Teller surface area (BET).....	45
3.3.5. Scanning electron microscopy (SEM).....	46
Conclusions	48
Acknowledgements	49
References	49
Chapter 4: Effect of torrefied wood biomass under an oxidizing atmosphere on downdraft gasification process.....	55
Abstract.....	55
4.1. Introduction.....	56
4.2. Materials and methods	58

4.2.1. Model description.....	58
4.2.2. Model validation.....	60
4.2.3. Wood analyzed	61
4.3. Results and discussion	62
4.3.1. Model validation.....	62
4.3.2. Effect of biochar production and fuel/air equivalence ratio	64
4.3.3. Effect of torrefaction under an oxidizing atmosphere	69
Conclusions	74
Acknowledgements	75
References	75
Recommendations for future study.....	79
Appendix A. Correlation to estimate the hardgrove grindability index (HGI)	80
References	81
Appendix B. Engine fuel quality (EFQ) deduction	82
References	84

List of Tables

Table 2.1. Torrefaction conditions and severity factor (SF).....	12
Table 2.2. TGA method for proximate analysis	14
Table 2.3. Chemical properties of raw and torrefied patula pine	21
Table 3.1. Chemical composition of raw and torrefied patula pine	36
Table 3.2. Infrared indices	44
Table 3.3. BET analysis for raw and torrefied patula pine.....	45
Table 4.1. Equations and equilibrium reaction of the thermodynamic model	59
Table 4.2. Experimental data used for model validation, adapted from [32].	60
Table 4.3. Chemical composition and heating value of raw and torrefied patula pine	61
Table 4.4. RMSE values for model validation.	63
Table A.1. Experimental data reported in literature	80
Table A.2. Results of the ANOVA.....	81

List of Figures

Figure 2.1. Experimental setup.....	11
Figure 2.2. Mass yield	16
Figure 2.3. Energy yield	17
Figure 2.4. Energy-mass co-benefit index.....	18
Figure 2.5. Physical properties of raw and torrefied patula pine chips	19
Figure 2.6. Physical changes occurred during torrefaction of patula pine wood chips	20
Figure 2.7. Chemical properties and composition of pine under the different torrefaction conditions	22
Figure 2.8. FVI changes for torrefied pine regarding the raw material.....	24
Figure 2.9. FVI and EMCI for raw and torrefied patula pine.....	25
Figure 3.1. DTG curves for raw and torrefied patula pine	38
Figure 3.2. TG parameters of different torrefaction conditions	40
Figure 3.3. FTIR spectra for raw and torrefied patula pine.....	41
Figure 3.4. SEM images of raw and torrefied patula pine.....	47
Figure 4.1. Model validation using torrefied wood gasification data reported by Bibens [32]	63
Figure 4.2. Reaction temperature of gasification [°C] for raw and torrefied pine in function of biochar production (Factor “i”) and Fr.....	65
Figure 4.3. Autothermal zones in gasification process.....	66
Figure 4.4. CGE [%] for raw and torrefied pine in function of biochar production (Factor “i”) and Fr.....	67
Figure 4.5. CO/CO ₂ ratio for raw and torrefied pine in function of biochar production (Factor “i”) and Fr	68
Figure 4.6. Reaction temperature	70
Figure 4.7. PG composition and heating value for raw and torrefied pine wood.....	71
Figure 4.8. CGE for raw and torrefied pine wood.....	72
Figure 4.9. EFQ and fuel/air stoichiometric ratio of PG for raw and torrefied pine wood ..	73

Acknowledgements

To God.

To my family for their encouragement and solid support, especially my parents (Luz Amparo and Silvio) and my brother Juan who have been there all the time.

To Professor Juan Fernando for sharing part of his life and knowledge with me during these fruitful years.

To Sebastián Delgado for his valuable support for the development of the first part of this investigation and for his valuable friendship.

To all the people who at the 20-349 office for those years. Special thanks to Hernán, Juan Pablo, and William for their kind help in the whole process.

To my friends Hugo, Camilo, Sebastián Duque, Fabián, Sebastián Heredia, Juan Carlos, Alex with who I shared great moments in the university during these years.

Chapter 1: Study of fixed bed gasification process of torrefied wood biomass under an oxidizing atmosphere

1.1. Introduction

The study of non-conventional energy sources such as biomass has grown worldwide. Global warming and the high dependence of fossil fuels in energy market are the issues that have favored the development of new energy conversion technologies [1]. Biomass is the non-conventional resource most used for energy production due to its high and decentralized availability compared with other sources as solar, wind and hydropower [2]. Particularly, wood biomass has a great energy potential in Colombia. The country has around 17 million ha of land available for forest commercial projects that can be used for energy crops [3]. Energy crops offer great advantages like they can establish in soils that are not suitable for agriculture purposes; which makes these crops sustainable [4]. This situation promotes an ideal field to promote the energy generation from biomass or to produce biofuels or bioproducts.

For producing chemicals, solid or liquid biofuels from biomass, it is necessary to guarantee that biomass has high heating value, low moisture and ash contents. However, in most cases, wood biomass does not accomplish with these criteria due to its natural state; which is characterized by high moisture content, low bulk and energy densities, and high power consumption for milling [5], [6]. These aspects constitute different challenges that wood biomass must overcome, such as high transportation costs, short storage periods due to fast decomposition by fungal [7]. Several upgrading strategies such as torrefaction have been implemented to improve wood biomass properties as a solid fuel.

Torrefaction is a thermochemical process conducted in inert environments (e.g. Nitrogen) at temperatures ranging from 200 to 300 °C [5], [6]. Torrefied biomass has higher heating value due to the reduction of moisture content and O/C ratio, better grindability properties, and hydrophobic nature compared with the raw material [8]–[13]. To conduct the torrefaction process under an inert atmosphere leads to higher operating costs because of the production and/or acquisition of the carrier gas [7], [14], [15]. The

reduction of operating costs can be achieved using air as a carrier gas and to conduct an oxidative torrefaction [7]. On the other hand, one of the thermochemical processes in which torrefied wood biomass can be used as feedstock is gasification. Gasification is a process that converts a solid feedstock into a gaseous fuel through its partial oxidation with a gasifying agent; e.g. air, pure oxygen, or water vapor [16]. The producer gas can be burned to generate power in turbines or internal combustion engines, or used for the production of value-added chemicals [17].

In this work, it is studied what the effect of torrefaction conditions under an oxidizing atmosphere on wood biomass properties and gasification process is. Chapter 2 presents the effect of torrefaction temperature and residence time on physicochemical properties of patula pine. Furthermore, several parameters are evaluated in order to determine the properties of torrefied pine as solid fuel. In chapter 3, thermal behavior, and changes in chemical structure and morphology of torrefied patula pine at different conditions is studied. Finally, chapter 4 evaluates the effect of torrefied pine on fixed bed gasification process using a model in thermochemical equilibrium.

This study pretends to give an answer to the following research questions: What is the effect of the torrefaction process under an oxidizing atmosphere on gasification process? What is the effect of torrefaction temperature on physicochemical properties of patula pine? Which is the best torrefaction condition under the experimental conditions of this study? And how do the chemical structure and morphology of patula pine change with the torrefaction process under an oxidizing atmosphere?

1.2. Research objectives

General objective

To evaluate the effect of torrefaction process under an oxidizing atmosphere on woody biomass properties seeking its application in the fixed bed gasification process.

Specific objectives

- To evaluate the physicochemical properties of torrefied wood biomass under an oxidizing atmosphere as a function of different torrefaction temperatures and residence times.

- To characterize, by means of a model in thermochemical equilibrium, the fixed bed gasification process of torrefied wood biomass under an oxidizing atmosphere from an energy point of view.

1.3. Contribution of this dissertation

With the development of the present study, it is pretended to contribute to the knowledge about the phenomena involved that combines upgrading strategies of biomass as solid biofuel and its performance in the fixed bed gasification process. Likewise, it seeks to generate impact in the following sectors:

- **Scientific impact**

A Master of Science with solid knowledge in the fields of energy and materials science to serve the university and the country is formed. The research line of energy exploitation of biomass will be strengthened in the GIMEL group, and scientific capacities of the Universidad de Antioquia will be consolidated.

- **Economic impact**

The economic sector would benefit due to more local knowledge about biomass upgrading technologies, gasification process, and the different phenomena involved can impulse their development in the country. With the research and development of local technology, the costs of its implementation would reduce. Likewise, by exploiting the forest potential of the country, from the energy-sustainable point of view, it is promoted the creation of new jobs for the inhabitants of the rural regions. Moreover, in the case of developing a biofuels market, this will contribute to the gross domestic product (GDP) of the country. This thesis also contributes to developing new methodologies for recover residual biomass from sawmills, giving an added value to this waste and making more sustainable the forest industry.

- **Socio-environmental impact**

To contribute the improvement of solid biofuels, this will allow developing strategies for sustainable energy crops as part of a global bioenergy market. In this sense, the feedstock and its upgrading processing technologies can be developed at national level. Biomass production under sustainable criteria will also contribute to the establishment of forest

plantations. As a consequence, new employments in rural areas for the inhabitants will be created. Furthermore, these crops can be established on degraded lands which are not apt for food production and will prevent that the latter be in danger due to planting timber by the new growing bioenergy market.

1.4. Authorship of peer review publications

Below are presented the research outcomes that have been published after peer review.

1.4.1. Journal articles

- **S. Ramos-Carmona**, J. F. Pérez, M. R. Pelaez-samaniego, R. Barrera, and M. Garcia-perez, “Effect of torrefaction temperature on properties of Patula Pine,” *Maderas. Cienc. y Tecnol.*, 2017. – Accepted

1.4.2. International congress

- J. F. Pérez, **S. Ramos**, and R. Barrera, “Análisis energético y exergético como herramienta de selección de biomasa como materia prima para la producción de biosyngas para motores de combustión,” in *X Congreso Nacional y V Internacional de Ciencia y Tecnología del Carbón y Combustibles Alternativos– CONICCA*, 2015, pp. 247–253.
- **S. Ramos-Carmona**, M. R. Peláez-Samaniego, and J. F. Pérez, “Characterization of pyrolysis products of torrefied biomass with dendroenergy potential in Colombia,” in *Sixth International Symposium on Energy from Biomass and Waste*, 2016. – Accepted
- J. F. Pérez, **S. Ramos-Carmona**, and A. Agudelo, “The impact of climate phenomenon ‘El Niño’ on energy cost and opportunities for bioenergy in Colombia,” in *Sixth International Symposium on Energy from Biomass and Waste*, 2016. – Accepted
- Y. Lenis, **S. Ramos-Carmona**, and J. F. Pérez, “Efficiency and flame front velocity in function of physical properties of biomass under gasification regimes in fixed bed,” in *Sixth International Symposium on Energy from Biomass and Waste*, 2016. – Accepted

References

- [1] Y. A. Lenis, A. F. Agudelo, and J. F. Pérez, “Analysis of statistical repeatability of a fixed bed downdraft biomass gasification facility,” *Appl. Therm. Eng.*, vol. 51, pp. 1006–1016, 2013.

- [2] R. H. H. Ibrahim, L. I. Darvell, J. M. Jones, and A. Williams, "Physicochemical characterisation of torrefied biomass," *J. Anal. Appl. Pyrolysis*, vol. 103, pp. 21–30, 2013.
- [3] J. F. Pérez and L. F. Osorio, *Biomasa forestal como alternativa energética: Análisis silvicultural, técnico y financiero de proyectos*. Medellín: Universidad de Antioquia, 2014.
- [4] B. Phalan, "The social and environmental impacts of biofuels in Asia: An overview," *Appl. Energy*, vol. 86, no. SUPPL. 1, pp. S21–S29, 2009.
- [5] M. Phanphanich and S. Mani, "Impact of torrefaction on the grindability and fuel characteristics of forest biomass," *Bioresour. Technol.*, vol. 102, no. 2, pp. 1246–1253, 2011.
- [6] T. G. Bridgeman, J. M. Jones, a. Williams, and D. J. Waldron, "An investigation of the grindability of two torrefied energy crops," *Fuel*, vol. 89, no. 12, pp. 3911–3918, 2010.
- [7] K. M. Lu, W. J. Lee, W. H. Chen, S. H. Liu, and T. C. Lin, "Torrefaction and low temperature carbonization of oil palm fiber and eucalyptus in nitrogen and air atmospheres," *Bioresour. Technol.*, vol. 123, pp. 98–105, 2012.
- [8] G. Xue, M. Kwapinska, W. Kwapinski, K. M. Czajka, J. Kennedy, and J. J. Leahy, "Impact of torrefaction on properties of *Miscanthus × giganteus* relevant to gasification," *Fuel*, vol. 121, pp. 189–197, 2014.
- [9] B. Arias, C. Pevida, J. Feroso, M. G. Plaza, F. Rubiera, and J. J. Pis, "Influence of torrefaction on the grindability and reactivity of woody biomass," *Fuel Process. Technol.*, vol. 89, no. 2, pp. 169–175, 2008.
- [10] M. Strandberg, I. Olofsson, L. Pommer, S. Wiklund-Lindström, K. Åberg, and A. Nordin, "Effects of temperature and residence time on continuous torrefaction of spruce wood," *Fuel Process. Technol.*, vol. 134, pp. 387–398, 2015.
- [11] L. D. Mafu, H. W. J. P. Neomagus, R. C. Everson, M. Carrier, C. A. Strydom, and J. R. Bunt, "Structural and chemical modifications of typical South African biomasses during torrefaction," *Bioresour. Technol.*, vol. 202, pp. 192–197, 2016.
- [12] L. E. Arteaga-Pérez, C. Segura, D. Espinoza, L. R. Radovic, and R. Jiménez, "Torrefaction of *Pinus radiata* and *Eucalyptus globulus*: A combined experimental and modeling approach to process synthesis," *Energy Sustain. Dev.*, vol. 29, pp. 13–23, 2015.
- [13] V. Repellin, A. Govin, M. Rolland, and R. Guyonnet, "Energy requirement for fine grinding of torrefied wood," *Biomass and Bioenergy*, vol. 34, no. 7, pp. 923–930, 2010.

- [14] S. Saadon, Y. Uemura, and N. Mansor, "Torrefaction in the Presence of Oxygen and Carbon Dioxide: The Effect on Yield of Oil Palm Kernel Shell," *Procedia Chem.*, vol. 9, pp. 194–201, 2014.
- [15] W. H. Chen, K. M. Lu, S. H. Liu, C. M. Tsai, W. J. Lee, and T. C. Lin, "Biomass torrefaction characteristics in inert and oxidative atmospheres at various superficial velocities," *Bioresour. Technol.*, vol. 146, no. x, pp. 152–160, 2013.
- [16] J. D. Martínez, K. Mahkamov, R. V. Andrade, and E. E. Silva Lora, "Syngas production in downdraft biomass gasifiers and its application using internal combustion engines," *Renew. Energy*, vol. 38, no. 1, pp. 1–9, 2012.
- [17] D. Baruah and D. C. Baruah, "Modeling of biomass gasification: A review," *Renew. Sustain. Energy Rev.*, vol. 39, pp. 806–815, 2014.

Chapter 2: Physicochemical characterization of torrefied wood biomass under an oxidizing atmosphere – Effect of temperature and residence time

Sergio Ramos Carmona, Sebastián Delgado Balcázar, Juan F. Pérez

Abstract

In this work, the effect of torrefaction under an oxidizing atmosphere on physicochemical properties of patula pine wood chips is studied. Raw and torrefied pine were characterized to evaluate the effect of temperature and residence time on biofuel properties such as bulk density, grindability (HGI), ultimate and proximate analyses, heating value, and fuel value index (FVI). On the other hand, torrefaction process was characterized by mass and energy yields, and by the energy-mass co-benefit index (EMCI). Torrefaction was carried out in a rotary kiln at temperatures between 180 and 240 °C during residence times between 30 and 120 minutes. Torrefaction process under an oxidizing atmosphere tends to increase the fixed carbon/volatile matter ratio (from 0.19 to 2.5) while decrease both H/C and O/C atomic ratios (from 1.54 to 0.41, from 0.73 to 0.33, respectively). The best properties of wood reached in the experimental plan were obtained at 210 °C during 75 minutes. For this torrefaction condition, energy yield, FVI, and EMCI are 85.91%, 1.91 kJ/cm³, and 4.41%, respectively. Additionally, lower heating value for torrefied pine (18.65 MJ/kg) is higher than for raw material (17.76 MJ/kg), and HGI is 17 % greater which results in better grindability behavior.

Keywords: Torrefaction, oxidizing atmosphere, Patula pine wood chips, physicochemical characterization.

2.1. Introduction

The increase in greenhouse gasses emissions have promoted the use of renewable energies such as biomass [1]. Forest biomass highlights for its potential due to its great and

decentralized availability; and can be used as feedstock to produce bioenergy and/or bioproducts (thermochemical biorefinery applications) [2]. Furthermore, forestry crops, by means of photosynthesis, mitigate CO₂ emissions produced during combustion of biomass. This fact aids to achieve the goals proposed during the COP21 – Paris 2015 to face the greenhouse emissions issue [1]–[3]. The use of biomass as feedstock for thermochemical or manufacture processes produces power, fuels for transport, chemical products, and materials that provide an alternative to fossil fuels such as coal, oil, and natural gas [4]. Therefore, the use of wood biomass as a renewable energy source contributes to energy diversification, besides enabling the production of a great variety of byproducts.

Biomass shows several disadvantages regarding fossil fuels (e.g. coal) due to its low bulk and energy densities [5], [6]. Therefore, large amounts of biomass are needed to satisfy a given energy demand. Moreover, wood biomass has high moisture content, which difficult its grinding, and storage due to degradation by fungal [7]. As strategies to improve and to homogenize wood biomass properties for thermochemical processes (e.g. combustion, co-firing with coal, gasification, and pyrolysis), it is feasible to implement upgrading processes such as torrefaction [5], [8], [9].

Torrefaction is a mild-pyrolysis process at low-middle temperatures (200–300°C) during different residence times (commonly less than 1h) under an inert atmosphere [10]. During torrefaction process, the heating value of biomass increases due to the reductions in moisture content, and H/C and O/C ratios [6]. Furthermore, torrefied biomass becomes hydrophobic due to the thermal degradation of hemicellulose. Hydrophobic nature of torrefied biomass allows extending storage periods [7]. Thereby, pretreated biomass exhibits better properties as biofuel than raw material.

In the state of the art, it has been reported that after torrefaction, the elemental composition of biomass tends to be similar to char composition [11]. Nevertheless, despite the advantages that offer a torrefied biomass, torrefaction increases the operation costs due to the cost associated with the inert gas supply (e.g. nitrogen) as carrier gas [12]. Among the strategies to reduce the costs related to the carrier gas, it is to perform the torrefaction under an oxidizing atmosphere using air as carrier gas instead of nitrogen [13].

Different authors have studied the effect of the use of air as carrier gas on the torrefaction process performance. Rousset et al. [14] studied the effect of oxygen

concentration in the carrier gas on the torrefaction process. Oxygen concentrations were 2, 6, 10, and 21 % vol.; with torrefaction temperatures of 240 and 280 °C for 1h of residence time. Authors stated that oxygen concentration does not significantly affect the composition of the solid by-product for low torrefaction temperatures. Therefore, they recommend to use an inert atmosphere for torrefaction temperatures above 280 °C to avoid oxidation of volatiles released during the process. Similarly, Wang et al. [15] analyzed the effect of temperature and oxygen concentration on torrefaction process. Oxygen increases degradation rates of hemicellulose leading to diminishing residence times. Moreover, energy consumption during torrefaction decreases due to the heat released as a consequence of oxidation reactions of volatiles with the carrier gas.

Other authors have evaluated the effect of temperature and particle size on torrefied biomass properties. Lu et al. [12] studied the effect of carrier gas type (inert and oxidizing) and temperature on characterization of oil palm fiber and eucalyptus. Palm fiber is not suitable for oxidative torrefaction, since its high surface/volume ratio enhances mass losses during upgrading process, which leads to lower energy yields. For eucalyptus, air can be used as the carrier gas during torrefaction but at lower temperatures. Uemura et al. [16] obtained that particle size does not have a significant effect on mass yield. They stated that this parameter depends on hemicellulose content in biomass, which is the wood constituent more affected during torrefaction process.

Chen et al. [13], [17], [18] carried out different studies of torrefaction process varying biomass type, carrier gas and its superficial velocity, and temperature. Unlike Uemura et al. [16], Chen et al. reported that under an oxidizing atmosphere, thermal degradation of wood highly dependent on particle size; i.e. surface area of the treated material. Likewise, as the oxygen concentration in the carrier gas increases, H/C ratio decreases due to oxygen reacts more readily with hydrogen than with carbon. Oxygen concentration does not affect fixed carbon content if torrefaction temperature is below 300 °C. This result agrees with the findings reported by Wang et al. [15].

Despite the wide research about torrefaction using air as carrier gas described above, there is a lack of information about the effect of the oxidizing environment on physical properties (e.g. bulk density, grindability) and fuel properties different to heating value of wood biomass. The objective of this study is to analyze the effect of torrefaction

temperature and residence time under an oxidizing atmosphere (air) on physicochemical and fuel properties of patula pine wood chips. Raw and torrefied materials are characterized by means of bulk density, hardgrove grindability index (HGI), proximate and ultimate analyses, and fuel value index (FVI). Additionally, torrefaction process is characterized by mass and energy yields, and energy-mass co-benefit index (EMCI). A complete characterization of raw and torrefied material will allow identifying the importance of strategies to upgrade the quality of wood biomass as biofuel (e.g. torrefaction) to further thermochemical processes applications under a low-cost atmosphere (air).

2.2. Materials and methods

2.2.1. Experimental setup

Experiments were carried out in a batch rotary kiln showed in Figure 2.1. The drum (5) is coupled to a variable speed drive system composed of a sprocket-chain system and an electrical worm gear reducer (9, 10, and 11). Reactor capacity ranges 2 – 3 kg regarding biomass bulk density. Electrical resistors (13) heat the reactor, where the temperature is measured by a K-type thermocouple (T1) and adjusted by a PID controller (12). K-type thermocouple (T2) measures the temperature outside the reactor to be sure that torrefaction temperature is reached. Carrier gas flow (i.e. air) is provided by a reciprocating compressor (1) coupled to a plenum (2) to absorb piston oscillations. Pressure and flow are regulated/measured by means of a manometer (3) and a rotameter (4), respectively. The reactor is isolated with a ceramic wall (7) and an air chamber (8) to avoid high heat transfer rates to the surroundings. Biomass samples are fed in a sample holder (6) to control the initial and final amount of biomass during the torrefaction process. Sample holder consists of a stainless steel tube (internal diameter 82.55 mm and length 170 mm) covered by a mesh of 0.149 mm size; the mesh allows to drag the released volatile matter during torrefaction by the carrier gas.

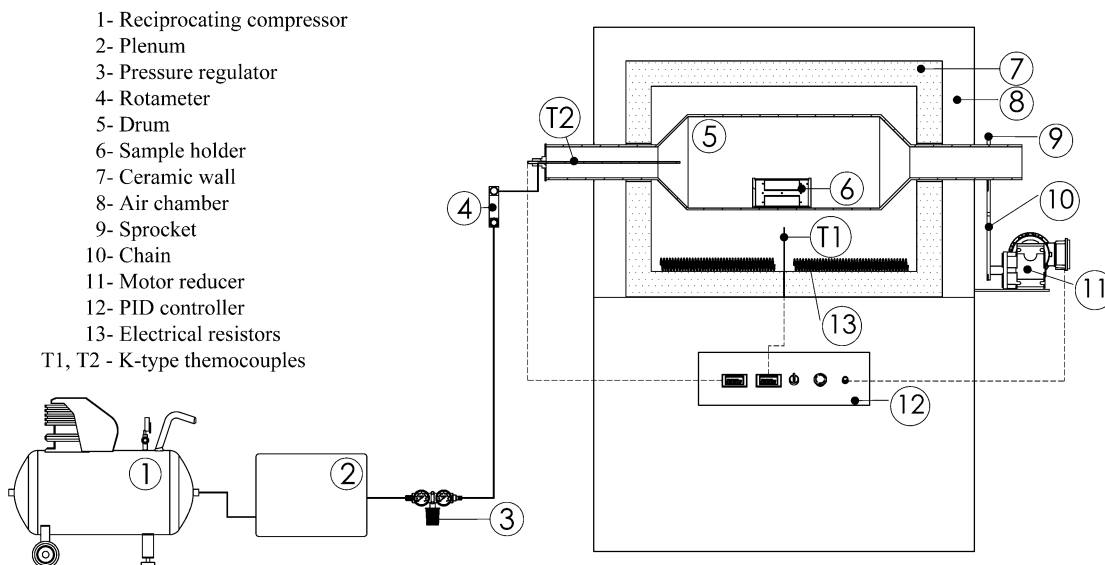


Figure 2.1. Experimental setup

2.2.2. Biomass as feedstock

Nowadays, Colombia produces around 10.4 m³ millions of wood for domestic consumption exclusively. This wood volume represents the 80% of the national production. Unfortunately, the majority of these crops come from natural forests which do not meet sustainability criteria [19]. On the other hand, the country has a potential of 17 million ha with forestry aptitude. Antioquia, Caldas, and Córdoba are the states with the biggest forest planted areas for commercial purposes under sustainability criteria. In these planted areas, the most common species are pines (*Pinus patula* and *Pinus tecunumanii*), and cedar (*Cupressus lusitánica*) [20]. Besides its large planted area, patula pine has a high Mean Annual Increment (MAI, ~ 20 m³/ha/year) and low harvested time (13 years). Small diameter logs were debarked before a chipping process. The wood sample was chipped using a Bandit 95XP chipper, then located on the floor (trying to keep a uniform thickness layer of chips) and dried at room conditions during two weeks. Then, the wood chips were sieved and classified by size between 10 and 20 mm since some thermochemical processing technologies (e.g. fixed bed gasification or combustion) operates with this particle size range [21]. This particulate size was used to conduct the experimental plan described below.

2.2.3. Experimental plan

The torrefaction tests were conducted with 50 g ($\pm 2\%$) of patula pine wood chips. The heating method was programmed with a heating rate of 10 °C/min and the residence time started once target temperature was reached. Air flow fixed in the experiment was 1 slpm to obtain a superficial velocity of 0.82 cm/min inside the reactor. Low superficial velocities of the carrier gas allow to obtaining high mass yields during torrefaction process [17]. Torrefaction temperatures were varied from 180 to 240 °C. Joshi et al. [22] reported ignition zones of biomass under different oxygen concentrations. For an oxygen concentration of 21 %vol. (air), the ignition zone is close to 240 °C. Residence time varied from 30 to 120 minutes. Table 2.1 shows the experimental conditions conducted in this work.

Table 2.1. Torrefaction conditions and severity factor (SF)

Sample	Temperature [°C]	Residence time [min]	SF	Test code
1	180	030	3.83	180-300
2		075	4.23	180-750
3		120	4.43	180-120
4	210	030	4.72	210-300
5		075	5.11	210-750
6		120	5.32	210-120
7	240	030	5.60	240-300
8		075	6.00	240-750
9		120	6.20	240-120

Additionally, a severity factor (SF) is introduced, which quantifies torrefaction severity combining temperature and residence time. Eq. 2.1 shows how to determine the severity factor of a torrefaction condition, as stated by Na et al. [23].

$$SF = \log \left\{ t \times \exp \left(\frac{T_{torr} - T_r}{14.75} \right) \right\} \quad (2.1)$$

Where t is the residence time in minutes, T_{torr} and T_r are the torrefaction temperature and a reference temperature in °C, respectively. T_r is often 100 °C [23]. It is considered that a temperature above 100 °C promotes not only moisture evaporation but also the release of volatile matter present in the wood. After torrefaction process, pine wood chips were ground and sieved using a 35–mesh to further characterization.

2.2.4. Torrefaction process characterization

2.2.4.1. Mass yield

Mass yield (m_y) is a measure of the remaining amount of biomass after torrefaction process and is determined by Eq. 2.2 [24]. m_{raw} and m_{torr} are the initial and final mass of material after torrefaction process in grams. Torrefaction process was conducted by triplicate.

$$m_y[\%] = \frac{m_{torr}}{m_{raw}} \cdot 100 \quad (2.2)$$

2.2.4.2. Energy yield

Energy yield (E_y) indicates how much energy conserves the biomass after torrefaction process regarding the initial energy content in the material [24]. This parameter involves mass and heating value changes as shown in Eq. 2.3. LHV_{raw} and LHV_{torr} are the initial and final lower heating value of biomass after torrefaction process in kJ/kg.

$$E_y[\%] = \frac{m_{torr} \cdot LHV_{torr}}{m_{raw} \cdot LHV_{raw}} \cdot 100 = m_y \cdot \frac{LHV_{torr}}{LHV_{raw}} \quad (2.3)$$

2.2.4.3. Energy-mass co-benefit index

The energy-mass co-benefit index (EMCI) was proposed by Lu et al. [12] to quantify the enhancement of energy content of the remaining mass after torrefaction process. EMCI is the difference between the energy and mass yields (Eq. 2.4). In other words, the EMCI is the product between mass yield and heating value gained with torrefaction process.

$$EMCI = E_y - m_y = m_y \left(\frac{LHV_{torr}}{LHV_{raw}} - 1 \right) \quad (2.4)$$

2.2.5. Biomass physicochemical characterization

In order to determine how the torrefaction under an oxidizing atmosphere affects the physicochemical properties of patula pine, the following characterizations were carried out.

2.2.5.1. Bulk density of biomass

Bulk density (ρ_{bulk}) is defined as the ratio between the mass of a material and its volume, including the void volumes of internal pores [25]. To determine this parameter, a vessel with known volume (V_{vessel}) is filled with the biomass, and it is weighted to estimate the mass change (m_{bms}). Eq. 2.5 allows calculating the bulk density of the different samples. For each condition, the procedure was conducted five times.

$$\rho_{bulk} \left[\frac{kg}{m^3} \right] = \frac{m_{bms}}{V_{vessel}} \quad (2.5)$$

2.2.5.2. *Hardgrove grindability index*

Several gasification and combustion technologies (fluidized or entrained reactors) require pulverized biomass as feedstock; therefore, it is important to know the effect of torrefaction process on biomass grindability behavior [5]. Hardgrove grindability index (HGI) is used to classify the grindability of several coals [26]. However, it is performed an equivalent adaptation valid to char and biomass as reported by Bridgeman et al. [27] and Ibrahim et al. [28]. HGI is estimated by means of correlation in function of biomass composition. An analysis of variance (ANOVA) was conducted taking into account experimental data of HGI in function of ultimate and proximate analyses [27]–[30]. According to the ANOVA, the proximate analysis has a more significant effect than ultimate analysis on HGI. Therefore, a correlation to estimate the HGI in function of proximate analysis was determined, as shown in Eq. 2.6, with a $R^2=0.93$. Volatile matter (VM) and ash contents of biomass are in wt. % on a dry basis.

$$HGI = 1147.05 + 0.149 \cdot VM^2 - 20.775 \cdot VM - 82.213 \cdot ash + 0.931 \cdot MV \cdot ash \quad (2.6)$$

2.2.5.3. *Proximate analysis*

Proximate analysis of each sample was determined by means of a thermogravimetric analyzer TA Instruments Q50. The method to conduct the analysis proposed by Medic et al. [31] was modified taking into account the ASTM D 3174-12 standard to determine the ash content [32]. The modified TGA method is presented in Table 2.2.

Table 2.2. TGA method for proximate analysis

Step	Procedure
0	Start with high purity N ₂ (100 ml/min)
1	Ramp 10 °C/min to 105 °C
2	Isothermal for 15 minutes
3	Ramp 10 °C/min to 900 °C
4	Isothermal for 10 minutes
5	Equilibrate at 750 °C
6	Change to zero air (100 ml/min)
7	Isothermal for 20 minutes

2.2.5.4. *Ultimate analysis*

A CHNSO LECO Truspec micro equipment was used to estimate the ultimate analysis of samples. Tests were conducted according to the ASTM D 5373-08 standard [33].

Carbon, hydrogen, and nitrogen analyses were carried out in a helium environment at 1050 °C; whereas oxygen content was determined by difference. Tests were conducted by triplicate.

2.2.5.5. Lower heating value

Heating value relates the energy release per unit mass of fuel. Higher heating value (HHV) of raw and torrefied biomass were determined by the correlation proposed by Friedl et al. [34] and shown in Eq. 2.7. Several authors used this correlation in other torrefaction studies due to its accuracy ($R^2=0.935$) [28], [35], [36].

$$HHV \left[\frac{kJ}{kg} \right] = 3.55C^2 - 232C - 2230H + 51.2(C \times H) + 131N + 20600 \quad (2.7)$$

Where C, H, and N are the carbon, hydrogen, and nitrogen contents from the ultimate analysis in wt. % on a dry basis, respectively. In order to observe the effect of torrefaction process on the heating value of biomass, lower heating value (LHV) was used in the study. To calculate the LHV, enthalpy of vaporization of water produced by hydrogen present in biomass is subtracted from the HHV [37].

2.2.5.6. Fuel value index

The fuel quality of biomass torrefied at different temperatures and residence times is quantified by means of the fuel value index (FVI). This parameter is a measure of the global properties of biomass as solid biofuel. It relates important properties such as heating value, bulk density, and ash and moisture contents [38]–[40].

$$FVI \left[\frac{kJ}{cm^3} \right] = \frac{LHV_{torr} [kJ/kg] \cdot \rho_{bulk} [kg/cm^3]}{\%H_2O \cdot \%ash} \quad (2.8)$$

2.3. Results and discussion

2.3.1. Torrefaction process characterization

2.3.1.1. Mass yield

Figure 2.2 shows the mass yield of patula pine for the different torrefaction conditions. For torrefied material at 180 °C, the mass yield is around 88% regardless the residence time of the experiment. Mass losses associated with these torrefaction conditions are attributed mainly to biomass drying and the release of low-molecular-weight volatiles [12]. When torrefaction temperature increases to 210 °C, mass losses increase with residence time,

being more notable between 30 and 75 minutes. At the most severe temperature condition (i.e. 240 °C), mass losses are greater than 60%. This behavior is obtained because, between 210 and 240 °C, oxidation reactions are activated leading to biomass carbonization [12], [9]. When residence time increases from 75 to 120 minutes, there is not have a significant effect on mass yield for the different torrefaction temperatures evaluated. Chen et al. [41] reported similar behavior for torrefied biomass under an inert atmosphere. By means of TGA analysis, they showed that the mass loss during torrefaction process at 240 and 275 °C is stabilized after 60 minutes of residence time. Lu et al. [12] reported similar results for the mass yield for torrefied eucalyptus under an oxidizing atmosphere. However, the similar mass yields were reached at a higher temperature (325 °C). It is due to the geometries used in their study were blocks of 10x15x20 mm; which have a lower surface/volume ratio than wood chips. Greater surface areas improve heat and mass transfer during torrefaction process leading to higher mass losses in the torrefied material. Several authors have stated that surface oxidation is the dominant phenomenon in torrefaction under an oxidizing atmosphere, which leads to higher mass losses in torrefied wood chips [15]–[17].

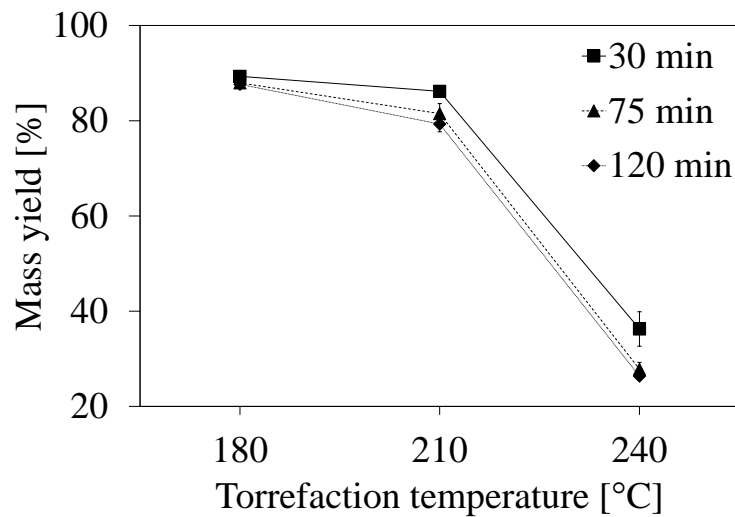


Figure 2.2. Mass yield

2.3.1.2. Energy yield

Figure 2.3 shows the effect of torrefaction process on energy yield. For torrefaction conditions of 180 °C during 30 and 75 minutes, it can be seen that energy yield is quite similar. This behavior is attributed to the balance between heating value gains and mass losses during torrefaction process (see Figure 2.2 and Table 2.3). At 180 °C, increasing

residence time up to 120 minutes leads to an increase in the energy yield of torrefied patula pine. At this torrefaction temperature, mass yield does not change meaningfully, while heating value increases due to changes in chemical composition of pine (see section 2.2.3). For torrefied patula pine at 210 °C, energy yield diminishes when residence time increases. A higher residence time enhances mass losses that cannot be compensated by the heating value increase. The lowest energy yields are reached when torrefaction temperature is 240 °C due to higher mass losses favored by the degradation of wood biomass by the oxidation reactions. Regarding residence time, torrefaction during 30 minutes leads to the highest energy yield for 240 °C as torrefaction temperature. This behavior is due to a lower residence time avoids high thermal degradation of biomass; therefore, less energy is released during torrefaction.

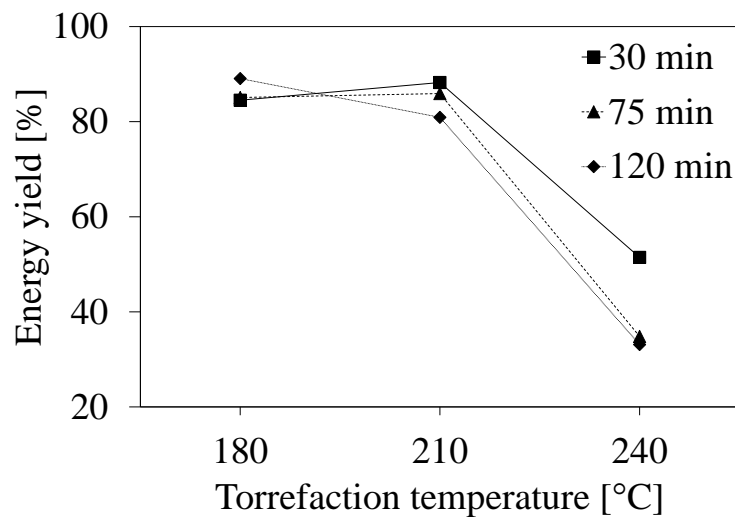


Figure 2.3. Energy yield

Unlike this study, Chen et al. [13] obtained greater energy yields although they conduct torrefaction experiments at higher temperatures than 240 °C (45 °C higher approximately). Results reported by these authors can be associated with differences in biomass particle sizes and experimental setup. On the other hand, similar results to our work are reported by Lu et al. [12], who obtained low energy yields (around 36.5%) for torrefied eucalyptus at temperatures that favored carbonization of the material (350 °C).

2.3.1.3. Energy-mass co-benefit index

Figure 2.4 shows the relative change of the EMCI for the different torrefaction conditions regarding the raw material (baseline). It can be observed that torrefaction at 180

°C during 30 and 75 minutes has a negative effect on the EMCI; which is associated with the non-significant change in the LHV regarding raw pine. At these torrefaction conditions, torrefied pine exhibits small changes in its elemental composition. For the other torrefaction conditions (210 °C and 240 °C), it is obtained a positive effect on the EMCI. Torrefied pine at 210 °C leads to a relative increase in the EMCI values up to 4.5%; which can be explained by a more noticeable heating value gain that overcomes the mass losses during torrefaction process. The highest relative increase of the EMCI (approximately 16% higher regarding raw pine) is reached for torrefied pine at 240 °C during 30 minutes. This increase is associated with the higher carbon content for pretreated pine at this condition (see section 2.2.2). If residence time increases for this temperature condition, the EMCI relative increase is lower due to oxidation reactions favored during torrefaction at 240 °C.

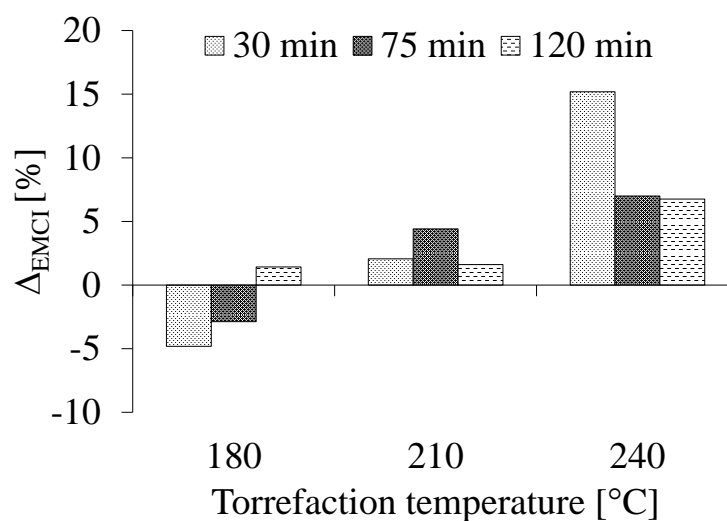


Figure 2.4. Energy-mass co-benefit index

2.3.2. Physicochemical characterization of torrefied biomass

2.3.2.1. Physical properties: bulk density and grindability

Figure 2.5a shows the bulk densities of raw and torrefied patula pine. In general, bulk density tends to diminish with increasing torrefaction temperature. Nevertheless, at 180 °C, there are not significant differences regarding the raw material when residence time increases. At this torrefaction temperature, low mass losses occur (around 10%, see Figure 2.2) and are mainly associated with biomass drying instead of volatiles release [42]. When torrefaction is carried out at 210 °C, the bulk density of torrefied pine tends to decrease (5 to 10%). At this temperature, mass losses become more considerable (14 and 20%, see

Figure 2.2) as a consequence of the thermal degradation of wood constituents (e.g. holocellulose) [14]. Additionally, biomass particle size does not change significantly. Thereby, the synergy of these phenomena leads to lower bulk densities of pretreated material.

The lowest bulk densities are obtained at 240 °C. The density of pretreated pine reaches values around the 30% of the raw material bulk density. This result is attributed to the higher mass losses during torrefaction process due to thermal degradation of wood constituents and by the carbonization reactions favored at this temperature condition. For this torrefaction temperature, it is expected a severe or complete thermal degradation of wood constituents; namely hemicellulose and cellulose. Furthermore, fixed carbon of torrefied pine decreases with residence time for this torrefaction temperature as described in section 2.3.2.2 leading to a reduction of the biomass particle size during torrefaction process. Thus, since the particle size decreases at 240 °C with residence time, bulk density increases, as can be seen in Figure 2.5a.

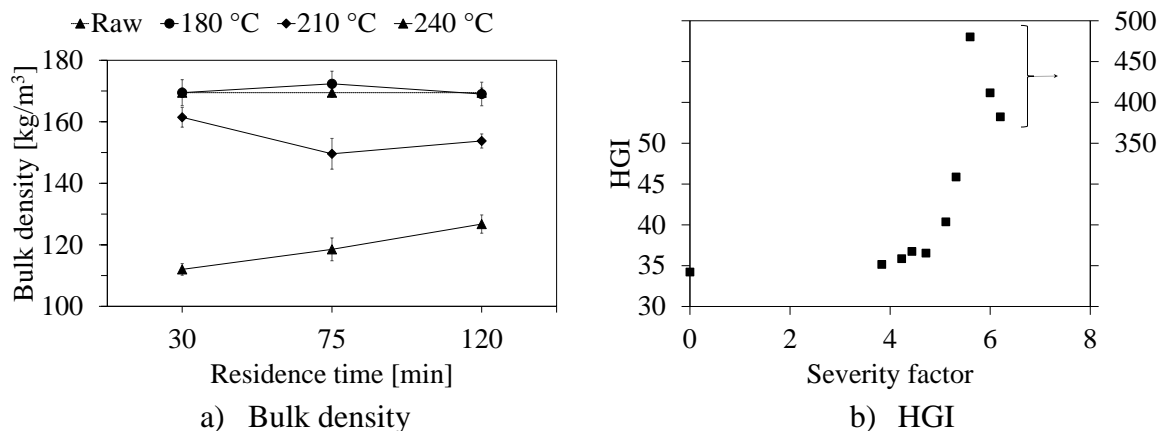


Figure 2.5. Physical properties of raw and torrefied patula pine chips

Figure 2.5b shows the HGI in function of the torrefaction severity factor (Table 2.1) in order to show the progressive change in the grindability behavior of the pretreated material. An increase in the process severity favors the grindability of pine wood chips, particularly in the most severe conditions (240 °C). Ohliger et al. [30] reported that biomass grindability increase when mass losses overcome the 30% due to thermal degradation of hemicellulose. A higher HGI is associated with lower energy consumption required to grind torrefied material [29]. Ibrahim et al. [28] presented values of HGI for different wood biomass torrefied at different temperature (270 and 290 °C) and time (30 and 60 minutes)

conditions under an inert atmosphere. Their results for torrefied eucalyptus (HGI=38.9–46.8) are similar to the results obtained in the present study.



Figure 2.6. Physical changes occurred during torrefaction of patula pine wood chips

Figure 2.6 shows physical changes occurred during torrefaction of patula pine wood chips at different pretreatment conditions. It can be seen how torrefaction severity affects the wood chips color. Torrefied pine at 240 °C has a char-like appearance due to the carbonization reactions occurred during the pretreatment. Changes in the color of torrefied materials result from the oxidation of phenolic compounds, presence of reduced sugars and amino acids, release of formaldehyde, and aromatization and polycondensation reactions [43].

2.3.2.2. *Composition and heating value*

Table 2.3 shows the proximate analyses for raw and torrefied patula pine at different pretreatment conditions. All torrefied samples at 180 °C and 210 °C during 30 minutes exhibit a slight decrease in their VM contents. At 210 °C, the release of VM increases with the residence time. A reduction of VM content leads to a relative increase of fixed carbon (FC) content in the torrefied materials. According to Rousset et al. [14], this release of volatiles is associated with the thermal degradation of cellulose due to the oxidizing environment during torrefaction process. This behavior differs with torrefaction under an inert atmosphere where the release of volatiles is mainly related to hemicellulose decomposition [41]. In this work it is obtained different results from those reported by Lu et al. [12] who also studied wood torrefaction under an oxidizing atmosphere. At 250°C,

they reported higher VM content (around 15%) than the concentration reached in this work at 240 °C. This difference is attributed to the higher size and shape of biomass studied by Lu et al.

Table 2.3. Chemical properties of raw and torrefied patula pine

Sample	Proximate analysis [wt.% db]			Moisture [wt.%]	LHV _{db} [MJ/kg]
	Volatile matter	Fixed carbon	Ash		
Raw	83.83	15.85	0.32	8.35	16.85
180-30	82.21	17.43	0.35	6.78	15.94
180-75	81.50	18.15	0.35	5.40	16.30
180-120	80.78	18.87	0.35	4.86	17.12
210-30	80.92	18.72	0.36	3.71	17.25
210-75	78.46	21.16	0.38	3.79	17.76
210-120	76.08	23.53	0.39	3.45	17.19
240-30	28.59	70.48	0.93	7.72	23.90
240-75	32.01	66.78	1.21	9.71	21.08
240-120	33.90	64.87	1.23	10.01	21.16

For torrefied pine at 240 °C, there is a considerable decrease of VM; which is associated with the severe or complete thermal degradation of the major wood constituents (i.e. hemicellulose and cellulose). During torrefaction at this temperature conditions, it is evidenced that oxidation reactions appear. Regarding FC content, the pretreated pine reaches concentrations about 70%. This composition is close to that of a biochar; thereby, these conditions are more associated with a carbonization process than a torrefaction one [12], [13]. Biomass carbonization has as result in an improvement in the heating value regarding the raw material [18]. Peláez-Samaniego et al. [43] reported a similar char-like material for a torrefaction process under an inert atmosphere. In this works, FC content of torrefied pine at 240 °C diminishes with increasing residence time. A longer residence time favors secondary oxidation reactions in the carbonaceous material, which affects the heating value negatively.

The effect of torrefaction severity on wood elemental composition is shown in Figure 2.7a. At 180 °C during 30 and 75 minutes, pine composition is quite similar to the raw material, since at these conditions the drying is the main subprocess favored. For other torrefaction conditions, the carbon content tends to increase (up to 40%) while hydrogen and oxygen contents tend to decrease (up to 66% and 37%, respectively) with torrefaction severity. At 240 °C, pine composition changes become greater; the highest carbon content

is obtained at this temperature for 30 minutes. However, at 240 °C, the carbon content diminishes with residence time due to the oxidation reaction.

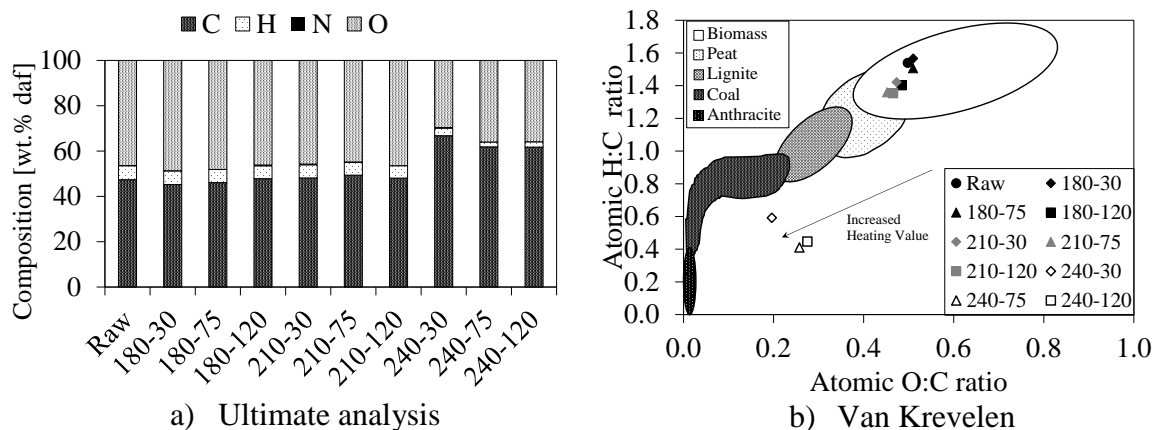


Figure 2.7. Chemical properties and composition of pine under the different torrefaction conditions

Another way to see the effect of torrefaction on patula pine composition is through the Van Krevelen diagram (Figure 2.7b). The figure shows the changes in the atomic H/C and O/C ratios for the different torrefaction conditions. Both ratios tend to decrease with torrefaction severity, especially for the most severe changes reached at 240 °C. The reductions of these atomic ratios are associated with the volatiles release due to the thermal degradation of wood constituents, that leads to an increase in the heating value of the torrefied pine (see Table 2.3) [11].

The atomic H/C ratio of torrefied biomass under an inert atmosphere tends to be higher than the obtained under an oxidizing atmosphere for the same temperature conditions [12]. This result is due to the thermal degradation of elements such as hydrogen and oxygen associated with the decomposition of wood constituents. The thermal degradation during torrefaction is favored by the oxidizing environment which leads to a relative increase in the carbon content of pretreated materials [12]; while for an inert atmosphere, it is required higher torrefaction temperatures to reach a reduction in the H/C ratio. For instance, in this work at 210 °C during 75 minutes (FS=5.11), it is obtained a reduction in the H/C ratio of 8%; whereas, under an inert atmosphere to reach a similar H/C reduction with ponderosa pine, it was required to pretreat the wood at 275 °C during 30 minutes (SF=15.3 according to Eq. 2.1) [43].

2.3.2.3. *Biomass properties as solid fuel*

LHV for raw and torrefied biomass is shown in Table 2.3. Torrefied pine at 180 °C during 30 and 75 minutes have a lower LHV than raw pine (around 5%). This reduction is mainly attributed to the error associated with the correlation used (Eq. 2.7) to estimate the HHV. For the other torrefaction conditions, this parameter tends to increase with torrefaction severity; this is attributed to the reduction of the H/C and O/C ratios (section 2.2.2.). The highest LHV was obtained for 240 °C and 30 minutes of residence time (23.9 MJ/kg). The increase in the heating value of torrefied biomass allows obtaining higher efficiencies in further thermochemical processes such as gasification, combustion, and pyrolysis [9].

Figure 2.8 shows the relative change in the FVI for the torrefied pine regarding the raw material (baseline). The most severe conditions (i.e. 240 °C) have a negative effect on pine wood chips as solid biofuel. The lower FVI is due to the drastic reduction in the bulk density (Figure 2.5a) that cannot be compensated by the higher heating value of these materials. Additionally, these samples have higher moisture contents because of the oxidation reactions that could produce water vapor during torrefaction process (see Table 2.3). On the other hand, at 180 °C, the biomass FVI tends to increase. Nevertheless, this enhancement is mainly attributed to biomass drying since bulk density, composition and heating value do not change meaningfully. Therefore, the best torrefaction conditions to obtain high-quality fuel are reached with a torrefaction temperature of 210 °C. These torrefaction conditions exhibit a considerable decrease in the moisture content (around 60%), and an increase in the LHV (around 5%); which compensates the lower bulk density and higher ash content regarding raw pine.

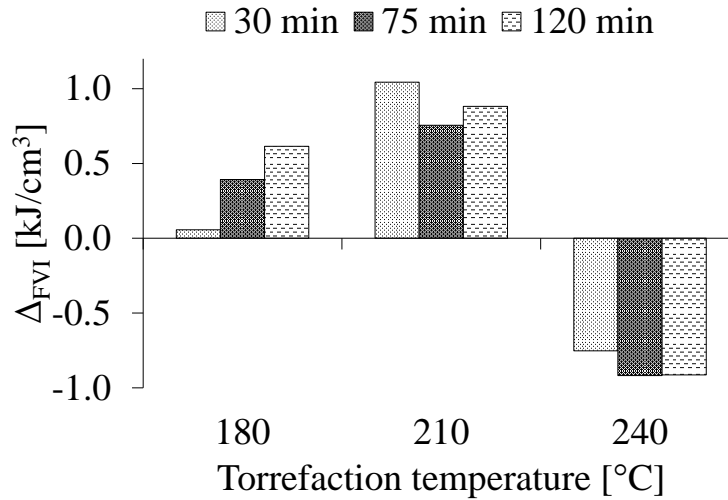


Figure 2.8. FVI changes for torrefied pine regarding the raw material

2.3.2.4. Methodology to select the best torrefaction conditions

In order to find the best torrefaction condition for this study, it is proposed to analyze the torrefaction process performance and the fuel quality of torrefied pine. Figure 2.9 shows the relation between FVI and EMCI for each torrefaction condition. Moreover, a hypothetical linear behavior of the two indices is presented; this ideal line shows that an increase in the EMCI leads to a proportional increase in the FVI or vice versa. Torrefaction of patula pine at 210 °C during 30 minutes is the condition that better adjust to the straight line, followed by torrefaction at 180 and 210 °C during 120 minutes. However, torrefaction at 210 °C during 75 minutes is the more suitable mode to upgrade patula pine. Despite this condition has a lower FVI (Figure 2.8), its EMCI is much greater than the obtained at 210 °C for 30 minutes (Figure 2.4). Therefore, according to the experimental plan conducted in this work, it is highlighted that to pretreat wood biomass (at 210 °C for 75 min) under oxidizing atmosphere leads to produce an upgraded biofuel with a FVI= 1.15 kJ/cm³ with a process improvement of 4.4%.

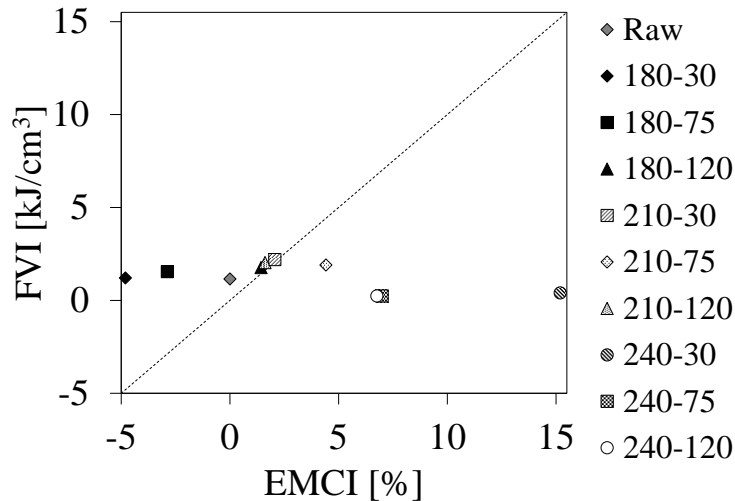


Figure 2.9. FVI and EMCI for raw and torrefied patula pine

Conclusions

Wood biomass torrefaction process conducted under an oxidizing atmosphere (air) represents a feasible option to upgrade biomass properties. Under the experimental conditions carried out in this work, the following conclusions can be drawn:

- The mass and energy yields of torrefied patula pine decrease with temperature. Mass losses can be above the 70% when torrefaction temperature is 240 °C due to hemicellulose and cellulose decomposition and by the oxidation reactions. Likewise, at 210 and 240 °C, these yields also decrease with residence time. The heating value gain due to the reduction of the H/C and O/C ratios does not compensate the higher mass losses to increase the energy yield.
- Physical properties of patula pine are affected by torrefaction severity (temperature and residence time). A higher torrefaction severity implies a reduction in the bulk density up to 40% regarding raw pine (170 kg/m³). On the other hand, grindability index improves considerably with torrefaction process. Torrefied pine at 240 °C has a HGI between 10 to 15 times greater than HGI for raw pine.
- To carry out a torrefaction process under an oxidizing atmosphere with severity factors below 4.72 (210 °C – 30 min) is not enough to cause significant changes in chemical composition of the pretreated material. This is because the volatiles release is not favored and hence, fixed carbon content of torrefied wood does not change

considerably. Torrefaction process at 240 °C favors the reduction of H/C and O/C ratios leading in a higher heating value, around 41% higher regarding the raw material.

- Torrefaction process at 210 °C during 75 minutes (SF=5.11) is an optimum condition to pretreat pine wood since this condition favors the improvement of torrefaction process (EMCI=4.41%) and the quality of wood as solid biofuel (FVI=1.15 kJ/cm³). Torrefied pine at this condition exhibits an energy yield of 85.91%, a heating value and HGI increase of 5% and 17% regarding raw pine, respectively.

Acknowledgements

The authors acknowledge Universidad de Antioquia for the financial support of this research through the projects “Estrategias de integración de la madera plantada en Colombia en conceptos de biorrefinería termoquímica: Análisis termodinámico y caracterización de bioproductos – PRG 2014-1016” and “Sostenibilidad 2015-2016”, and through the “Estudiante instructor” program. Also, authors acknowledge Centro de Investigaciones Ambientales y de Ingeniería (CIA) of the Universidad de Antioquia for the financial support through the CODI PR 15-2-09 project.

References

- [1] National Climatic Data Center (NOAA). “Global Analysis-Annual 2014,” 2015.
- [2] COMMISSION STAFF WORKING DOCUMENT, “State of play on the sustainability of solid and gaseous biomass used for electricity, heating and cooling in the EU,” Brussels, 2014.
- [3] (Organización de las Naciones Unidas) ONU, “Convención Marco sobre el Cambio Climático,” vol. 21930, p. 40, 2015.
- [4] U.S Energy Information Administration, “Biomass and the Environment,” 2015. [Online]. Available: http://www.eia.gov/Energyexplained/?page=biomass_environment.
- [5] M. Phanphanich and S. Mani, “Impact of torrefaction on the grindability and fuel characteristics of forest biomass,” *Bioresour. Technol.*, vol. 102, no. 2, pp. 1246–1253, 2011.
- [6] B. Arias, C. Pevida, J. Feroso, M. G. Plaza, F. Rubiera, and J. J. Pis, “Influence of torrefaction on the grindability and reactivity of woody biomass,” *Fuel Process. Technol.*, vol. 89, no. 2, pp. 169–175, 2008.

- [7] M. Hakkou, M. Pétrissans, P. Gérardin, and A. Zoulalian, "Investigations of the reasons for fungal durability of heat-treated beech wood," *Polym. Degrad. Stab.*, vol. 91, no. 2, pp. 393–397, 2006.
- [8] J. Deng, G. jun Wang, J. hong Kuang, Y. liang Zhang, and Y. hao Luo, "Pretreatment of agricultural residues for co-gasification via torrefaction," *J. Anal. Appl. Pyrolysis*, vol. 86, no. 2, pp. 331–337, 2009.
- [9] W. H. Chen, K. M. Lu, W. J. Lee, S. H. Liu, and T. C. Lin, "Non-oxidative and oxidative torrefaction characterization and SEM observations of fibrous and ligneous biomass," *Appl. Energy*, vol. 114, pp. 104–113, 2014.
- [10] W. H. Chen, P. C. Kuo, S. H. Liu, and W. Wu, "Thermal characterization of oil palm fiber and eucalyptus in torrefaction," *Energy*, vol. 71, pp. 40–48, 2014.
- [11] P. C. Bergman, R. Boersma, R. W. R. Zwart, and J. H. Kiel, "Torrefaction for biomass co-firing in existing coal-fired power stations," *Energy Res. Cent. Netherlands ECN ECNC05013*, no. July, p. 71, 2005.
- [12] K. M. Lu, W. J. Lee, W. H. Chen, S. H. Liu, and T. C. Lin, "Torrefaction and low temperature carbonization of oil palm fiber and eucalyptus in nitrogen and air atmospheres," *Bioresour. Technol.*, vol. 123, pp. 98–105, 2012.
- [13] W. Chen, K. Lu, W. Lee, S. Liu, and T. Lin, "Non-oxidative and oxidative torrefaction characterization and SEM observations of fibrous and ligneous biomass," *Appl. Energy*, vol. 114, pp. 104–113, 2014.
- [14] P. Rousset, L. MacEdo, J. M. Commandré, and A. Moreira, "Biomass torrefaction under different oxygen concentrations and its effect on the composition of the solid by-product," *J. Anal. Appl. Pyrolysis*, vol. 96, pp. 86–91, 2012.
- [15] C. Wang, J. Peng, H. Li, X. T. Bi, R. Legros, C. J. Lim, and S. Sokhansanj, "Oxidative torrefaction of biomass residues and densification of torrefied sawdust to pellets," *Bioresour. Technol.*, vol. 127, pp. 318–325, 2013.
- [16] Y. Uemura, W. Omar, N. Aziah, S. Yusup, and T. Tsutsui, "Torrefaction of oil palm EFB in the presence of oxygen," *Fuel*, vol. 103, pp. 156–160, 2013.
- [17] W. H. Chen, K. M. Lu, S. H. Liu, C. M. Tsai, W. J. Lee, and T. C. Lin, "Biomass torrefaction characteristics in inert and oxidative atmospheres at various superficial velocities," *Bioresour. Technol.*, vol. 146, no. x, pp. 152–160, 2013.

- [18] W. H. Chen, Y. Q. Zhuang, S. H. Liu, T. T. Juang, and C. M. Tsai, "Product characteristics from the torrefaction of oil palm fiber pellets in inert and oxidative atmospheres," *Bioresour. Technol.*, vol. 199, pp. 367–374, 2016.
- [19] J. F. Pérez and L. F. Osorio, *Biomasa forestal como alternativa energética*. Medellín: Universidad de Antioquia, 2014.
- [20] ProExport, "Sector Forestal en Colombia," Conif, pp. 1–17, 2012.
- [21] J. F. Pérez, A. Melgar, and P. N. Benjumea, "Effect of operating and design parameters on the gasification/combustion process of waste biomass in fixed bed downdraft reactors: An experimental study," *Fuel*, vol. 96, pp. 487–496, 2012.
- [22] Y. Joshi, M. Di Marcello, E. Krishnamurthy, and W. De Jong, "Packed-Bed Torrefaction of Bagasse under Inert and Oxygenated Atmospheres," *Energy and Fuels*, vol. 29, no. 8, pp. 5078–5087, 2015.
- [23] B. Il Na, B. J. Ahn, and J. W. Lee, "Changes in chemical and physical properties of yellow poplar (*Liriodendron tulipifera*) during torrefaction," *Wood Sci. Technol.*, vol. 49, no. 2, pp. 257–272, 2014.
- [24] W.-H. Chen, J. Peng, and X. T. Bi, "A state-of-the-art review of biomass torrefaction, densification and applications," *Renew. Sustain. Energy Rev.*, vol. 44, pp. 847–866, 2015.
- [25] M. L. d. Souza-Santos, *Solid Fuels Combustion and Gasification - Modeling, Simulation, and Equipment Operation*. New York: Marcel Dekker, Inc., 2004.
- [26] ASTM, "D409/D409M-11a: Standard Test Method for Grindability of Coal by the Hardgrove-Machine Method," *Annu. B. ASTM Stand.*, vol. 54, pp. 1–14, 2012.
- [27] T. G. Bridgeman, J. M. Jones, a. Williams, and D. J. Waldron, "An investigation of the grindability of two torrefied energy crops," *Fuel*, vol. 89, no. 12, pp. 3911–3918, 2010.
- [28] R. H. H. Ibrahim, L. I. Darvell, J. M. Jones, and A. Williams, "Physicochemical characterisation of torrefied biomass," *J. Anal. Appl. Pyrolysis*, vol. 103, pp. 21–30, 2013.
- [29] O. Williams, C. Eastwick, S. Kingman, D. Giddings, S. Lormor, and E. Lester, "Investigation into the applicability of Bond Work Index (BWI) and Hardgrove Grindability Index (HGI) tests for several biomasses compared to Colombian la Loma coal," *Fuel*, vol. 158, pp. 379–387, 2015.

- [30] A. Ohliger, M. Förster, and R. Kneer, "Torrefaction of beechwood: A parametric study including heat of reaction and grindability," *Fuel*, vol. 104, pp. 607–613, 2013.
- [31] D. Medic, M. Darr, A. Shah, B. Potter, and J. Zimmerman, "Effects of torrefaction process parameters on biomass feedstock upgrading," *Fuel*, vol. 91, no. 1, pp. 147–154, 2012.
- [32] ASTM International, "ASTM D 3174-12: Standard Test Method for Ash in the Analysis Sample of Coal and Coke from Coal," West Conshohocken, PA, USA, 2012.
- [33] ASTM, "D5373-08 Standard Test Methods for Instrumental Determination of Carbon, Hydrogen, and Nitrogen in Laboratory Samples of Coal," *Annu. B. ASTM Stand.*, vol. 5, no. October 2002, pp. 1–9, 2012.
- [34] A. Friedl, E. Padouvas, H. Rotter, and K. Varmuza, "Prediction of heating values of biomass fuel from elemental composition," *Anal. Chim. Acta*, vol. 544, no. 1–2 SPEC. ISS, pp. 191–198, 2005.
- [35] M. Wilk, A. Magdziarz, and I. Kalembe, "Characterisation of renewable fuels' torrefaction process with different instrumental techniques," *Energy*, vol. 87, pp. 259–269, 2015.
- [36] Y. Zhang, A. Yao, and K. Song, "Torrefaction of cultivation residue of *Auricularia auricula-judae* to obtain biochar with enhanced fuel properties," *Bioresour. Technol.*, vol. 206, pp. 211–216, 2016.
- [37] Y. Cengel and M. E. Boles, "Termodinámica", p. 1456, 2011.
- [38] A. N. Purohit and A. R. Nautiyal, "Fuelwood Value Index of Indian Mountain Tree Species," *Int. Tree Crop. J.*, vol. 4, no. 2–3, pp. 177–182, 1987.
- [39] S. Ojelel, T. Otiti, and S. Mugisha, "Fuel value indices of selected wood fuel species used in Masindi and Nebbi districts of Uganda," *Energy. Sustain. Soc.*, vol. 5, no. 1, p. 14, 2015.
- [40] C. A. Cuvilas, *Mild Wet Torrefaction and Characterization of Woody Biomass from Mozambique for Thermal Applications*. 2015.
- [41] W. H. Chen and P. C. Kuo, "A study on torrefaction of various biomass materials and its impact on lignocellulosic structure simulated by a thermogravimetry," *Energy*, vol. 35, no. 6, pp. 2580–2586, 2010.

[42] T. Oliveira Rodriguez and P. Rousset, “Effects of torrefaction on energy properties of eucalyptus grandis wood,” *Statew. Agric. L. Use Baseline* 2015, vol. 1, 2009.

[43] M. R. Pelaez-Samaniego, V. Yadama, M. Garcia-Perez, E. Lowell, and A. G. McDonald, “Effect of temperature during wood torrefaction on the formation of lignin liquid intermediates,” *J. Anal. Appl. Pyrolysis*, vol. 109, pp. 222–233, 2014.

Chapter 3: Chemical and structural changes in torrefied wood biomass under an oxidizing atmosphere

Sergio Ramos Carmona, Juan F. Pérez

Abstract

In this work, structure and morphology of patula pine wood chips torrefied under an oxidizing atmosphere are studied. Several analytical techniques were conducted to evaluate the changes in thermal behavior, chemical structure, surface area, and cell-wall structure of wood biomass at different torrefaction conditions. Torrefaction process was carried out in a rotary kiln varying the temperature (180, 210, and 240 °C) and residence time (30, 75 and 120 minutes). Torrefied wood biomass has higher reactivity due to the increase in its pore surface area and pore size; which may also improve the grindability behavior of the material. Furthermore, pretreated material structure exhibits higher aromaticity by the relative increase of lignin content leading to an enhancement in the heating value. Therefore, torrefaction under the oxidizing atmosphere improves the quality of pine wood as a solid biofuel for further thermochemical processing such as combustion or gasification. However, as a consequence of the thermal decomposition of cellulose, pyrolysis behavior may be affected.

Keywords: Torrefaction, oxidizing atmosphere, Patula pine chips, wood biomass, morphological characterization, FTIR, SEM, BET, TGA.

3.1. Introduction

Renewable energy sources have been utilized worldwide to mitigate the impact of global warming. Moreover, these resources have been promoted to diminish the high dependence of fossil fuels in the energy market [1]. Among several renewable alternatives for energy production is biomass, which is the most used due to its higher and decentralized availability compared with wind and solar energies [2]. Biomass has high moisture content which leads to fast fungal decomposition, low bulk and energy densities, and it requires

high power consumption for milling [2]–[4]. These characteristics contribute to decrease processing efficiencies and increase storage and transportation costs [5]. Upgrading strategies such as torrefaction have been implemented to improve biomass properties as solid biofuel. Torrefaction is a thermochemical process conducted in inert environments (e.g. Nitrogen) at temperatures ranging from 200 to 300 °C [2]–[4]. Torrefied biomass has higher heating value due to the reduction of moisture content and O/C ratio, better grindability properties, and hydrophobic nature compared with the raw material [6]–[11]. Using an inert atmosphere for torrefaction process implies higher operating costs because of the production and/or acquisition of the carrier gas [5], [12], [13]. The reduction of torrefaction operating costs can be achieved using air as a carrier gas to conduct an oxidative torrefaction [5]. However, an oxidizing atmosphere can promote oxidation reactions of the volatile matter released, and to oxidize the surface of the pretreated biomass [13], [14].

Several studies have been carried out in order to study the effect of the oxidizing atmosphere on the torrefaction process. Some of them have reported that oxygen concentration in the carrier gas did not affect the biomass composition, and mass and energy yields significantly [14], [15]. On the other hand, other authors such as Uemura et al. [16] reported that mass yield decreases with increasing torrefaction and oxygen concentration. Furthermore, they stated that oxidative torrefaction occurs in two successive steps; namely conventional torrefaction and oxidation. During conventional torrefaction, thermal degradation of biomass is related to cellulose decomposition instead of hemicellulose as occur in torrefaction process under an inert atmosphere [14]. For the oxidation stage, the CO₂ concentration in volatiles released increases leading to a reduction of the heating value of torrefied biomass [15]. This oxidation stage is favored by the carrier gas superficial velocity, which intensifies the mass and heat transfer in biomass during torrefaction process [13]. Regarding biomass type, authors have reported that oxidative torrefaction is a process suitable for lignocellulosic biomass, since its cell wall structure is relatively insensitive to the oxidative reaction [5], [17]. Torrefaction under an oxidizing atmosphere also improves heating value, hydrophobicity, and grindability behavior of pretreated material [18], [19]. Therefore, this process is suitable for upgrading wood biomass properties as solid biofuel reducing process operating costs. Nevertheless, despite

this process has been studied widely, a deeper study of the morphological and structural changes of biomass with oxidative torrefaction was not found in the literature cited as it occurs for the torrefaction process under an inert atmosphere [2], [9], [20], [21].

The aim of this work is to present a detailed study of the effect of torrefaction process under an oxidizing atmosphere (air) on the structure and morphology of a wood biomass. Different torrefaction temperatures (180, 210, and 240 °C) and residence times (30, 75, and 120 minutes) were conducted in a batch rotary kiln to obtain several torrefied materials. Raw and torrefied wood biomass were characterized through proximate and ultimate analyses, TGA, BET surface area, FTIR, and SEM to evaluate how the wood biomass is affected looking to produce an upgraded biofuel for further thermochemical processes.

3.2. Materials and methods

3.2.1. Materials

The raw material is patula pine wood (*Pinus patula*) obtained from a commercial timber sawmill located nearby Medellín, Colombia. The selection of this wood species took into account the silvicultural potential that pine offers in Colombian lands such as planted area (3849 ha), mean annual increment (MAI, 20 m³/ha/year) and harvested time (13 years) [22]. Small diameter logs were debarked before a chipping process. The wood sample was chipped using a Bandit 95XP chipper, then located on the floor (trying to keep a uniform thickness layer of chips) and dried at room conditions during two weeks. Then, the wood chips were sieved and classified by size between 10 and 20 mm. This range was selected due to it is the typical size of wood chips used in further thermochemical processes such as gasification and combustion (fixed bed), which allows obtaining an oxidation stage more stable [23], [24].

3.2.2. Experimental setup and torrefaction process

Torrefaction process was carried out in a batch rotary kiln of 2 kg capacity. A PID controller is used to adjust the temperature and heat rate according to the different torrefaction conditions. A detailed description of torrefaction facility is explained in chapter 2. Heat rate was fixed to 10 °C/min due to the objective of the study is not to evaluate the effect of this parameter on the torrefaction performance. The air flow was set at 1 slpm to obtain a low air superficial velocity. According to Chen et al. [13], higher mass yields in

the torrefaction process were reached with low air superficial velocities. Three levels of torrefaction temperatures (180, 210, and 240 °C) and three levels of residence time (30, 75, and 120 minutes) were evaluated. After torrefaction process, the materials were ground and sieved using a 35-mesh to perform its characterization. The experimental tests were coded as temperature-time, i.e. a code 180-30 corresponds to a test conducted at 180 °C for 30 minutes as residence time (section 3.3.3).

3.2.3. *Proximate and ultimate analyses*

Proximate and ultimate analyses were conducted to follow the changes in patula pine composition for the different torrefaction conditions. Proximate analysis procedure was based on the modification of the method proposed by Medic et al. [25]. On the other hand, ultimate analysis procedure followed the ASTM D 5373-08 standard [26]. A detailed description of the equipment and methodology utilized in the study is found in chapter 2.

3.2.4. *Analytical techniques*

Several instrumental techniques were performed to get a deeper insight of the changes in torrefied wood biomass under the oxidizing atmosphere. Among these techniques are TGA and FTIR analyses, BET surface area, and SEM images.

3.2.4.1. *Thermogravimetric analysis (TGA)*

TGA analysis was conducted in order to study the thermal behavior of raw and torrefied biomass. Analyses were carried out in a thermogravimetric analyzer TA Instruments Q50. The heating rate was 10 °C/min and the temperature varied from room conditions to 600 °C with a nitrogen flow of 100 ml/min. Approximately 10 mg ($\pm 2\%$) of material was employed in each case, and tests were conducted in duplicate to verify results. From DTG curves, two parameters were determined to describe the devolatilization temperature and reactivity of pretreated materials. The parameters are the base temperature and the reactivity factor, which are determined following the procedures described by Barrera et al. [27] and Ghetti [28], respectively.

The base temperature of material is defined as the temperature in which the DTG curve is equal to 1 %/min in the devolatilization stage [27]. Materials with higher base temperature are considered more thermally stables. The reactivity (R_a, min^{-1}) is defined

according to Eq. 3.1, where m_0 is the initial mass in the thermogravimetric test in mg, and DTG_{max} is the highest value of the DTG curve in mg/min [28].

$$R_a = \frac{1}{m_0} \cdot DTG_{max} \quad (3.1)$$

3.2.4.2. *Infrared spectroscopy characterization (FTIR)*

The changes in chemical structure of pine wood for the different torrefaction conditions were followed by FTIR analysis. For qualitative FTIR a KBr pellet was prepared at 2 wt.% of wood. A Shimadzu IRAffinity-1 spectrometer was used with a detector operated in a wavenumber range of 4000-400 cm^{-1} . Three measurements of each sample were taken to estimate the method repeatability.

3.2.4.3. *Brunauer–Emmett–Teller (BET) surface area*

The pore surface areas of the raw and torrefied patula pine were determined by gas adsorption isotherms using N_2 at $-196\text{ }^\circ\text{C}$ as adsorptive with a Micrometrics ASAP 2020 equipment. Samples were outgassed to 10 μmHg at $80\text{ }^\circ\text{C}$ during 8 h. The Brunauer–Emmett–Teller (BET) theory was applied to the N_2 adsorption data in the interval of relative pressure (P/P_0) 0.06–0.3 at 77 K. This analysis aims to determine the mesoporous surface area evolution for the different torrefaction conditions.

3.2.4.4. *Scanning electron microscopy (SEM)*

Changes in morphology of cell wall structure of raw and torrefied biomass were observed with SEM micrographs. A small amount of ground material for each torrefaction condition was previously covered with a gold film. Then, covered samples were placed in a JEOL JSM-6490 microscope operated at an accelerating voltage of 30 kV with a 40, 150 and 500 magnifications.

3.3. Results and discussion

3.3.1. *Proximate and ultimate analyses*

Table 3.1 shows the compositions and mass yields for the raw and torrefied patula pine. Mass yield is a measure of the remaining solid after torrefaction process, as explained in chapter 2. This parameter decreases when torrefaction temperature and residence time increases. Nevertheless, temperature has more effect than residence time. Indeed, the mass

yield does not change meaningfully when residence time increases from 75 to 120 minutes. Volatile matter content for pretreated material decreases with increasing torrefaction temperature up to 210 °C regardless residence time. This behavior is associated with the progressive thermal degradation of wood constituents (cellulose, hemicellulose); which decompose in a wide temperature range [14], [29]. Volatiles released have high O/C and H/C ratios; thereby, the hydrogen and oxygen contents of pretreated biomass decrease [5]. Therefore, for these torrefaction conditions (up to 210 °C) is obtained a relative increase in both fixed carbon and elemental carbon contents. For torrefied pine at 240 °C, its composition is quite similar to char composition. This is a consequence of the oxidation that patula pine suffers at this torrefaction temperature [5], [17]. When residence time increases, oxidation reactions prevail leading to a decrease in the fixed carbon and elemental carbon contents. Materials with high fixed carbon and elemental carbon contents have a better heating value favoring their quality as feedstock for further thermochemical processing (e.g. combustion, gasification) [23]. Chapter 2 presents a detailed study of the effect of torrefaction process under an oxidizing atmosphere on fuel properties of patula pine.

Table 3.1. Chemical composition of raw and torrefied patula pine

Torrefaction condition	Mass yield [%]	Ultimate analysis [wt. % daf ^a]				Proximate analysis [wt. % db ^b]		
		C	H	N	O	Volatile matter	Fixed carbon	Ash
Raw	-	55.70	7.14	0.19	36.97	83.83	15.85	0.32
180-300	89.47	55.15	7.20	0.15	37.50	82.22	17.43	0.35
180-750	87.79	55.40	6.96	0.00	37.64	81.49	18.15	0.36
180-120	87.55	56.45	6.60	0.48	36.47	80.78	18.87	0.35
210-300	86.07	56.91	6.74	0.44	35.91	80.92	18.72	0.36
210-750	80.30	58.15	6.59	0.22	35.04	78.46	21.16	0.38
210-120	78.36	57.68	6.51	0.00	35.81	76.08	23.53	0.39
240-300	34.19	76.03	3.75	0.35	19.87	28.59	70.48	0.93
240-750	27.04	72.58	2.49	0.02	24.91	32.01	66.78	1.21
240-120	26.56	71.17	2.65	0.08	26.10	33.90	64.87	1.23

^a dry ash free, ^b dry basis

3.3.2. Thermogravimetric analysis

Figure 3.1 shows the DTG of raw and torrefied pine wood to study their thermal behaviors. The curves for torrefied samples were multiplied by their respective mass yield (see Table 3.1) to establish a standard basis (i.e. raw basis) for comparison purposes, and to

follow the thermal degradation of wood constituents with torrefaction severity. This procedure followed the methodology that Pelaez-Samaniego et al. [30] used for a similar biomass (ponderosa pine) torrefied under an inert atmosphere (N₂). Raw pine exhibits a shoulder corresponding to hemicellulose decomposition at approximately 320 °C, and a peak related to cellulose degradation at 360 °C [29], [30]. Hemicellulose is the wood constituent mainly affected when torrefaction process is carried out under an inert atmosphere due to its thermal decomposition occurs between 150 and 350 °C [29]. On the other hand, when is present in the carrier gas during a torrefaction process, cellulose is the wood constituent that starts to decompose due to the enhancement of its thermal reactivity which accelerates the mass loss in the first stage of the process [14]. This behavior can be seen in the DTG curves of torrefied material where in the temperature range related to hemicellulose decomposition (150–350 °C), devolatilization of material still occurs [29]. For torrefied pine up to 210 °C during 120 minutes, if the torrefaction severity increases, the peaks associated with cellulose decrease and move towards lower temperatures. Peak shifting to lower temperatures implies changes in the structural characteristics of cellulose in torrefied patula pine due to depolymerization reactions that occur during torrefaction process [31]. Therefore, cellulose becomes a more reactive constituent due to these structural changes; i.e. its thermal decomposition occurs at lower temperatures. Hemicellulose is not affected severely with increasing torrefaction severity; this leads to a relative increase of this constituent in the pretreated materials. On the other hand, torrefied pine at 240 °C shows a different thermal behavior. At these torrefaction conditions, DTG curves are almost straight lines. A complete degradation of hemicellulose and cellulose occur at these conditions; which leads to obtaining a char-like material. Therefore, for this temperature condition is better to talk about a partial combustion process than a torrefaction one. A partially oxidized material is characterized by high fixed carbon and element carbon contents [17], which agrees with proximate and ultimate analyses of material treated at 240 °C (Table 1). For these materials, element carbon and fixed carbon range from 71–76% and 64–70 %, respectively. Pelaez-Samaniego et al. [30] obtained a similar thermal behavior when torrefied ponderosa pine under an inert atmosphere at 350 °C during 30 minutes. Thereby, it can be concluded that oxygen accelerates oxidation of the material during torrefaction process when the air is used as the carrier gas.

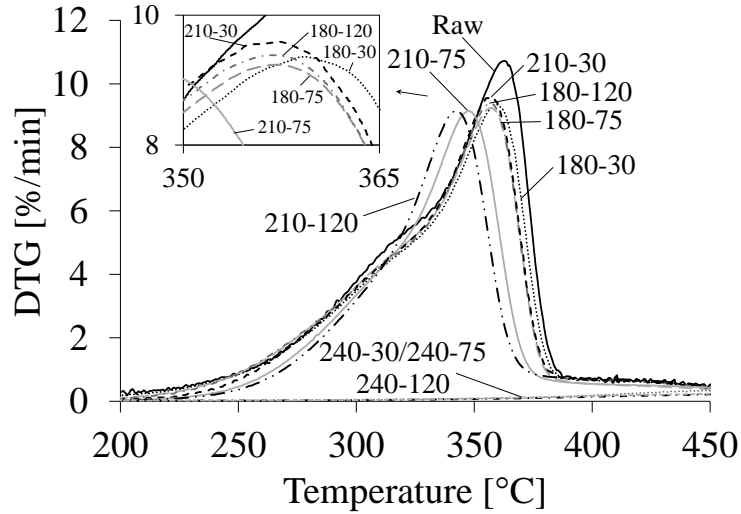


Figure 3.1. DTG curves for raw and torrefied patula pine

Figure 3.2a shows the base temperature, which is a measure of the start of the devolatilization stage for samples analyzed by the TGA; i.e. a higher base temperature is associated with a higher thermal stability. Volatile matter (VM) plays a key role in the devolatilization process of raw and torrefied biomass. For torrefied material at 180 °C, VM contents do not change at these torrefaction conditions meaningfully. As torrefaction severity increases from 210 °C and 30 minutes to 210 °C and 120 minutes, the base temperature increases while VM content decreases (Table 3.1). Therefore, the thermal stability of torrefied samples increases implying that a higher temperature is needed to start the devolatilization of a pretreated material at these conditions. Regarding torrefied biomass at 240 °C, base temperature tends to decrease with a residence time beyond 75 minutes. This behavior occurs because at this temperature condition, volatile matter increases with increasing residence time as explained before (see section 3.3.1.). Nevertheless, even though the devolatilization stage is delayed, its duration becomes shorter for torrefied material (i.e. treated material up to 210 °C during 120 minutes). Figure 3.1 shows how the temperature range in which devolatilization occurs becomes shorter with increasing torrefaction severity. This behavior is associated with the increase in the reactivity of torrefied material and the structural changes in wood constituents.

Figure 3.2b shows the relation between the reactivity and the VM:FC ratio of each sample. For torrefied material, reactivity tends to increase with severity degree despite VM content decreases. The release of volatile matter during torrefaction process leads to increase the porosity of torrefied wood, and hence their surface area (see sections 3.3.4. and

3.3.5.). A higher surface area increases the heat and mass transfer areas that favor a faster devolatilization process [32], [33]. For materials treated at 240 °C, reactivity decreases considerably due to the increase of fixed carbon regarding raw material (see Table 3.1). The increase of reactivity, with residence time for this temperature condition is associated with the higher VM contents and surface areas of samples treated during more time. As stated above, the increase of the VM content with the residence time of char-like material obtained at 240 °C is due to the oxidation reaction of fixed carbon with oxygen in the carrier gas. In general, reactivity for torrefied material during 180 and 210 °C does not change significantly regarding raw pine; which is suitable for the biofuel since a delayed volatiles release would reduce its reaction velocity in thermochemical processes such as gasification and/or combustion [23].

Since torrefaction under the oxidizing atmosphere decomposes cellulose structure instead of hemicellulose, it is expected that the behavior of pretreated material changes if they are used as feedstock in a thermochemical process such as pyrolysis. The main pyrolysis products from hemicellulose, cellulose, and lignin decomposition are acetic acid, levoglucosan, and phenolic compounds, respectively [34]–[37]. Then, it is expected that a bio-oil obtained from the pyrolysis of torrefied pine at low and medium temperatures (i.e. 180 and 210 °C) will have higher acetic acid and lower levoglucosan concentrations. This behavior is due to the relative increase of hemicellulose with torrefaction severity, which has acetyl groups that produce the acid [38]. Furthermore, the decomposition of cellulose and structural changes of this constituent with torrefaction would affect the production of the levoglucosan. Thereby, bio-oil will not have a good quality for bioethanol production, which needs high concentrations of levoglucosan, but can be used as feedstock to produce multiple high-value chemicals in few conversion steps [36], [37]. For a bio-oil from torrefied biomass under an inert atmosphere, several authors have reported an opposite behavior; i.e. pyrolysis bio-oil has higher levoglucosan and lower acetic acid concentrations due to the thermal decomposition of hemicellulose during torrefaction process [36]–[38].

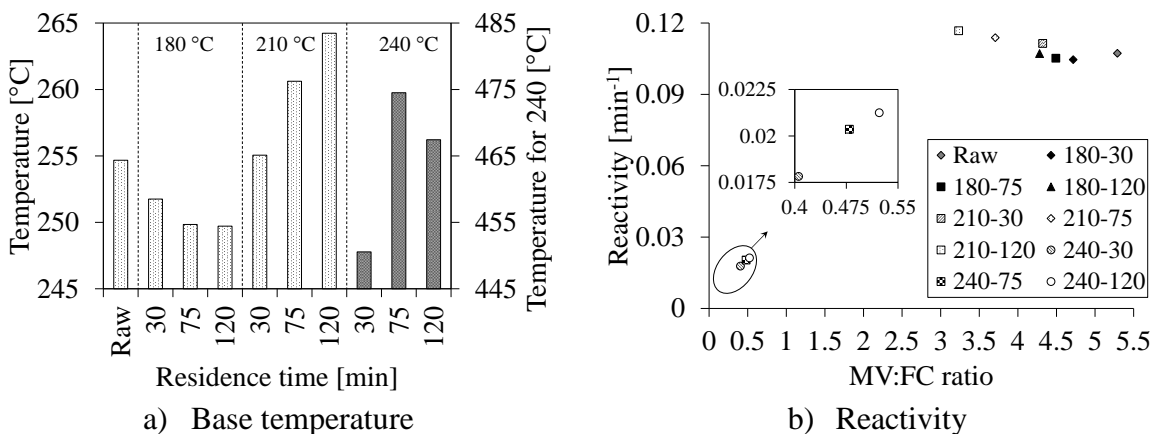


Figure 3.2. TG parameters of different torrefaction conditions

3.3.3. Infrared spectroscopy characterization (FTIR)

The analysis of FTIR was conducted by overlapping the spectra in the same baseline for comparison purposes. Figure 3.3 shows all FTIR spectra for raw and torrefied patula pine. This figure shows materials that are considered as torrefied (labeled as “Torrefaction” below raw spectrum) and partially oxidized (labeled as “Partial oxidation” above raw spectrum). In the range of 4000–2400 cm^{-1} , the OH stretching band (3450–3400 cm^{-1}) do not present significant changes in torrefied biomass at 180 °C during 30 minutes concerning raw material; which is in agreement with the proximate analysis of these materials where moisture, hydrogen, and oxygen contents change slightly (Table 3.1). When residence time increases to 75 and 120 minutes with torrefaction temperature of 180 °C, the OH bands diminish in intensity. This trend is attributed mainly to loss of water due to drying of biomass instead chemical reactions during torrefaction process. For torrefied materials at 210 °C, OH stretching band does not change almost in intensity but it does in shape. This band becomes broader since intramolecular hydrogen bondings and hydroxyl groups from phenols are detectable around 3300 cm^{-1} [39]. Phenolic compounds are related to lignin content present in biomass [30]. As mentioned before, biomass torrefied at 240 °C is subjected to greater oxidation reactions which result in a char-like material due to complete degradation of cellulose and hemicellulose [29], [30]. For these materials, it can be seen that the OH bands do not have a defined shape and show higher intensity regarding the raw pine. Oxidation of the pretreated material implies aromatization reactions that are identified in a wavenumber around 3050 cm^{-1} [21]. The occurrence of the new signal leads to the superposition of these peaks and hence, a straight line in the spectra of torrefied

samples at 240 °C is seen between 3300 and 3050 cm^{-1} . Increase in intensity of the OH bands at these torrefaction conditions may be due to a relative increase in lignin content and/or oxidation reactions presented under the experimental conditions; which could produce water on the surface of treated materials. Hydroxyl groups in biomass structure are related to its hydrophobic nature [2]. However, FTIR spectra do not give precise information about the loss or gain of these groups during these torrefaction conditions.

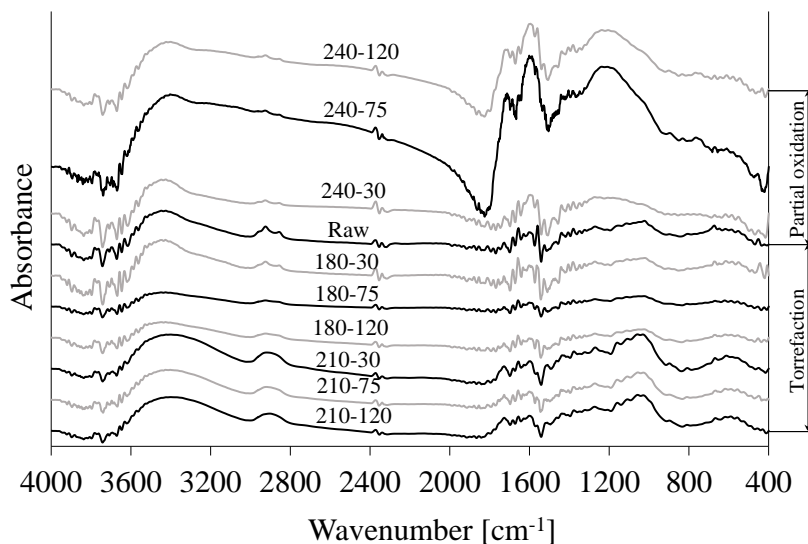


Figure 3.3. FTIR spectra for raw and torrefied patula pine

The range of 2950–2850 cm^{-1} corresponds to CH stretching vibrations assigned to aliphatic groups [21]. For torrefaction temperatures of 180 and 240 °C, this band tends to diminish with torrefaction severity, i.e. the bands decrease with increasing residence time. Reduction in peak intensities is due to the volatiles released during torrefaction process. According to the proximate analysis, the VM/FC ratio decreases with torrefaction severity (Table 3.1). For torrefied biomass at 210 °C, the peak related to asymmetrical stretching of methylene groups $-\text{CH}_2$ ($\sim 2936 \text{ cm}^{-1}$) is not shown defined as in the raw spectrum due to the increase in the intensity of the symmetrical stretching of methylene $-\text{CH}_2$ and methyl $-\text{CH}_3$ groups ($\sim 2860 \text{ cm}^{-1}$). Despite the release of volatiles, this band (CH stretching) does not diminish with residence time for this torrefaction temperature. Partial depolymerization of cellulose, which occurs at this torrefaction temperature, changes the structural characteristics of this constituent and increases the aliphatic groups in the torrefied material [40], [41].

The OH and CH bands are related to all wood constituents, i.e. cellulose, hemicellulose, and lignin [31]. Thereby, it is not possible to associate changes in these bands to a particular constituent. Modifications in the wood constituents due to torrefaction process can be seen in the bands ranged from 400 to 2000 cm^{-1} [31], [40]. Bands at about 1710–1740 cm^{-1} are related to the stretching vibrations of the C=O groups attributed to oxygen functionalities in non-conjugated and conjugated systems (carbonyl/carboxyl groups) of hemicelluloses [2], [21]. For torrefied biomass at 180 °C, peak intensity does not change significantly with increasing residence time. According to proximate and ultimate analyses, torrefied samples at this temperature show a quite similar composition to raw biomass. At 210 °C, torrefied materials at this temperature show higher intensity in the C=O band with increasing residence time. The increase in the intensity of this peak indicates a relative increase of the hemicellulose content in the torrefied material under the oxidizing atmosphere. This result is consistent with the DTG curves (Figure 3.1), where it is shown that the oxidizing atmosphere enhances cellulose decomposition instead of hemicellulose degradation during torrefaction process. For torrefaction process using inert atmosphere, different authors report that this signal tends to disappear due to the thermal degradation of hemicellulose caused by deacetylation during thermal treatment [2], [31], [42]. For biomass torrefied at 240 °C, the C=O signal increase in intensity with residence time and it is shifted to smaller wavenumbers. This behavior may be attributed to the increase of carbonyl or carboxyl groups in lignin by oxidation reactions [42].

The band at 1595 cm^{-1} corresponds to vibrations in the aromatic ring of lignin (C=C) plus C=O stretching [2], [42]. This peak increases with torrefaction severity (i.e. increasing temperature and residence time) which implies the higher aromaticity of torrefied biomass under oxidizing atmosphere due to the presence of more condensed guaiacyl units than etherified ones [31]. Torrefied materials at 240 °C show the highest intensities for this signal, which is in agreement with the behavior mentioned above related to the peak detected around 3050 cm^{-1} (aromatization reactions). Furthermore, this signal becomes broader suggesting an increase of structural diversity around the aromatic rings due to condensation reactions [42]. As well as the band at 1595 cm^{-1} ; the bands at 1508, 1430, and 1269 cm^{-1} are related to the lignin content of raw and torrefied materials. These signals correspond to C=C aromatic ring vibrations, C–H deformation in lignin and carbohydrates,

and C–O stretching and linkage in guaiacyl aromatic methoxyl group, respectively [2], [21], [31], [42]. In general, these signals tend to diminish and become broader with torrefaction severity; except for torrefied biomass at 240 °C where the band around 1260 cm^{-1} which increases markedly due to biomass partial oxidation. Therefore, torrefaction process under oxidizing atmosphere tends to modify lignin structure and increase its content, especially at higher temperatures where partial oxidation of the material occurs.

The bands at 1376, 1160, 1050, and 898 cm^{-1} are related to cellulose and hemicellulose content in biomass. They represent C–H deformation, C–O–C asymmetric stretching, C–O stretching vibrations, and C–H deformation in polysaccharides, respectively [21], [31], [42]. For torrefied biomass at 180 °C, no major changes are observed with the increase in residence time which agrees with proximate, ultimate and TGA analyses. C–H deformation and C–O stretching vibrations bands decrease slightly, whereas C–O–C asymmetric stretching and C–H deformations in polysaccharides bands do not change with residence time. When torrefaction temperature increases to 210 °C, FTIR spectra show great changes in the 1160 and 1050 cm^{-1} wavenumbers. The peak intensities are higher when residence time increases, especially for the peak at 1050 cm^{-1} as a consequence of the relative increase of hemicellulose. Peaks at 1376 and 898 cm^{-1} do not show major changes in these torrefaction conditions. Regarding torrefied biomass at 240 °C, these bands (1376, 1160, 1050, and 898 cm^{-1}) do not appear due to complete degradation of the constituents during torrefaction process. The peak that is seen around 1200 cm^{-1} is related to C–O stretching and linkage in guaiacyl aromatic methoxyl group as stated above. The band at 670 cm^{-1} is characteristic for cellulose and, it is associated with O–H torsional vibrations [43]. Peak intensity tends to diminish with torrefaction severity. This behavior aids to support the idea that torrefaction at 210 °C under an oxidizing atmosphere decomposes cellulose structure of biomass instead of hemicellulose [14].

Another way to verify the structural changes in torrefied biomass is through the infrared indices. These indices are described and used by Pohlmann et al. with the purpose of following the wood decay in function of torrefaction severity [21]. Torrefaction severity factor is determined as described in chapter 2. Table 3.2 shows the infrared indices calculated for the different torrefaction conditions. $I_{\text{ar}}/I_{\text{al}}$ and $I_{\text{C=Clig}}$ ratios determine the aromaticity and lignin maturity of torrefied biomass, respectively. On the other hand,

$I_{C=C}/I_{C=O}$ and I_{LIG}/I_{CHY} indicate the relative abundance of carbohydrates in the samples. The values of the different indices for the pretreated samples are used to compare with the raw material and determine changes in the fraction of the different wood constituents.

Table 3.2. Infrared indices

Torrefaction condition	Severity factor	I_{ar}/I_{al}	$I_{C=Clig}$	$I_{C=C}/I_{C=O}$	I_{LIG}/I_{CHY}
Raw	0.00	0.874	1.461	1.341	0.918
180-300	3.83	0.909	1.521	1.381	0.908
180-750	4.23	0.963	1.051	1.039	0.989
180-120	4.43	0.923	1.070	1.040	0.972
210-300	4.72	0.910	1.035	1.045	1.009
210-750	5.11	0.969	1.068	1.031	0.965
210-120	5.32	0.975	1.066	1.017	0.955
240-300	5.60	1.139	2.091	1.837	0.878
240-750	6.00	1.857	1.732	1.494	0.863
240-120	6.20	1.586	1.866	1.443	0.773

As expected, I_{ar}/I_{al} index confirms the slight increase of aromaticity in torrefied biomass up to 210 °C and a greater increase when torrefaction temperature is 240 °C due to partial oxidation of pretreated material. However, this index decreases for the torrefaction condition of 240 °C during 120 minutes due to oxidation reactions, which are favored with the residence time. $I_{C=Clig}$ and $I_{C=C}/I_{C=O}$ show similar behavior with torrefaction severity, i.e. the indices tend to diminish for torrefied material at 180 °C during 75 and 120 minutes and at 210 °C for all residence times. For torrefaction temperature of 240 °C, the indices are higher than those for raw biomass, but they decrease with the residence time that may enhance secondary reactions. On the other hand, I_{LIG}/I_{CHY} tends to increase slightly up to 210 °C and 30 minutes, and then diminish with higher torrefaction severity. These behaviors are associated with modifications in lignin structure and thermal decomposition of cellulose and hemicellulose during torrefaction process.

From an energy point of view, torrefaction process under an oxidizing atmosphere improves the quality of wood as feedstock for further thermochemical processes such as gasification or combustion. The reason is that thermal pretreatment enhances the abundance of C–O–C and C=C linkages in biomass structure due to the relative increase of hemicellulose and lignin. C–O–C and C=C linkages can release higher energy than other functional groups in biomass structure (e.g. C–O or C–H bonds); which implies the increase in energy density (i.e. heating value) of torrefied biomass [4], [44]. A higher

heating value in torrefied biomass allows reaching higher efficiencies in combustion and gasification processes [17]. The effect of torrefied wood on gasification process is presented in the chapter 4.

3.3.4. Brunauer–Emmett–Teller surface area (BET)

The aim of the BET analysis using N₂ as the adsorption gas is to follow the mesopore surface area with increasing torrefaction severity [21]. Table 3.3 shows the specific surface areas as well as pore volumes and pore sizes for the different torrefaction conditions. It can be seen that for raw and treated material up to 210 °C during 120 minutes (Severity factor between 0 and 5.32), the specific surface area and pore volume range from 3.0 to 7.0 m²/g and from 0.001 to 0.003 m³/g, respectively. These values are in agreement with those obtained by Pohlmann et al. [21], Ibrahim et al. [2], and Park et al. [45] for raw and torrefied biomass under an inert atmosphere. Therefore, oxygen present in the carrier gas during torrefaction process at low-middle temperatures do not have a significant effect on the porous structure of treated materials. For material treated at 240 °C, the specific surface areas are bigger due to the oxidation reactions that occur at this temperature condition.

Table 3.3. BET analysis for raw and torrefied patula pine.

Torrefaction condition	Severity factor	BET surface area [m ² /g] ^a	Pore volume [m ³ /g]	Pore size [Å]
Raw	0.00	4.66 (0.19)	0.0017	14.17
180-300	3.83	6.01 (0.12)	0.0020	13.23
180-750	4.23	6.62 (0.22)	0.0023	14.04
180-120	4.43	3.47 (0.23)	0.0012	13.76
210-300	4.72	6.54 (0.15)	0.0024	14.60
210-750	5.11	6.74 (0.14)	0.0023	13.92
210-120	5.32	4.01 (0.18)	0.0016	15.80
240-300	5.60	29.21 (0.57)	0.0144	19.72
240-750	6.00	174.94 (4.88)	0.0878	20.07
240-120	6.20	5.76 (0.11)	0.0020	14.22

^a Values in parenthesis are the corresponding standard deviations

Torrefaction processes at the different temperatures tend to increase the surface area (up to 44%) of treated materials when their residence time does not exceed 75 minutes. This behavior is attributed to the release of volatiles that occurs at these temperatures, which are mainly composed by H₂O and CO₂ [21], [46]. Furthermore, when increasing torrefaction severity (time from 30 to 75 minutes), volatiles with higher molecular weights start to release and may plug some pores forming new ones. This plugging complicates the porous

structure leading to increasing the surface area of the torrefied material [46]. The increase in the surface area leads to the enhancement in the reactivity of the torrefied material as shown in the TGA analysis (section 3.3.2).

On the other hand, once the residence time reaches 120 minutes, the surface area of the pretreated material decreases no matter the torrefaction temperature. As explained before (section 3.3.1), mass losses of treated material do not increase considerably when the residence time of torrefaction process increase from 75 to 120 minutes (see Table 3.1). Thereby, changes in surface area for this time conditions may be associated with secondary reactions between the oxygen, the volatiles released, and biomass during the torrefaction process (namely oxidation or depolymerization reactions). These reactions lead to the closure and restructuration of some mesopores, which results in a reduction of the specific surface area of the material. Chen et al. [46] reported similar behavior in the specific surface area of torrefied sawdust under an inert atmosphere. Likewise, treated materials (torrefied and oxidized) also have a microporous structure that can be enhanced due to the restructuration of the mesoporous one. The increase in microporous structure increases the surface area of the material. Pohlmann et al. [21] show that microporous surface areas for torrefied and carbonized pine are higher (around 20 and two times, respectively) than mesoporous ones. This behavior explains the higher reactivity of the material treated at 180 and 210 °C during 120 minutes regarding same temperature conditions during shorter residence times (section 3.3.2); even when the mesoporous surface area decreases (Table 3.3).

3.3.5. Scanning electron microscopy (SEM)

Scanning electron microscopy (SEM) was carried out to study the changes in morphology of patula pine in function of torrefaction severity. Figure 3.4 shows SEM images of raw and torrefied materials. It can be seen that morphology of patula pine does not change considerably with torrefaction severity up to 210 °C during 30 minutes. Materials have fibrous nature and particle sizes around 400 µm. Additionally, the pits in pine structure are similar and have a tend slightly to increase in size with torrefaction severity and becoming in one (white circles) obtaining bigger pores in the structure. Furthermore, the mass losses that occur at these torrefaction conditions aid to create new pores, which improve the specific surface area of treated material (see section 3.3.4).

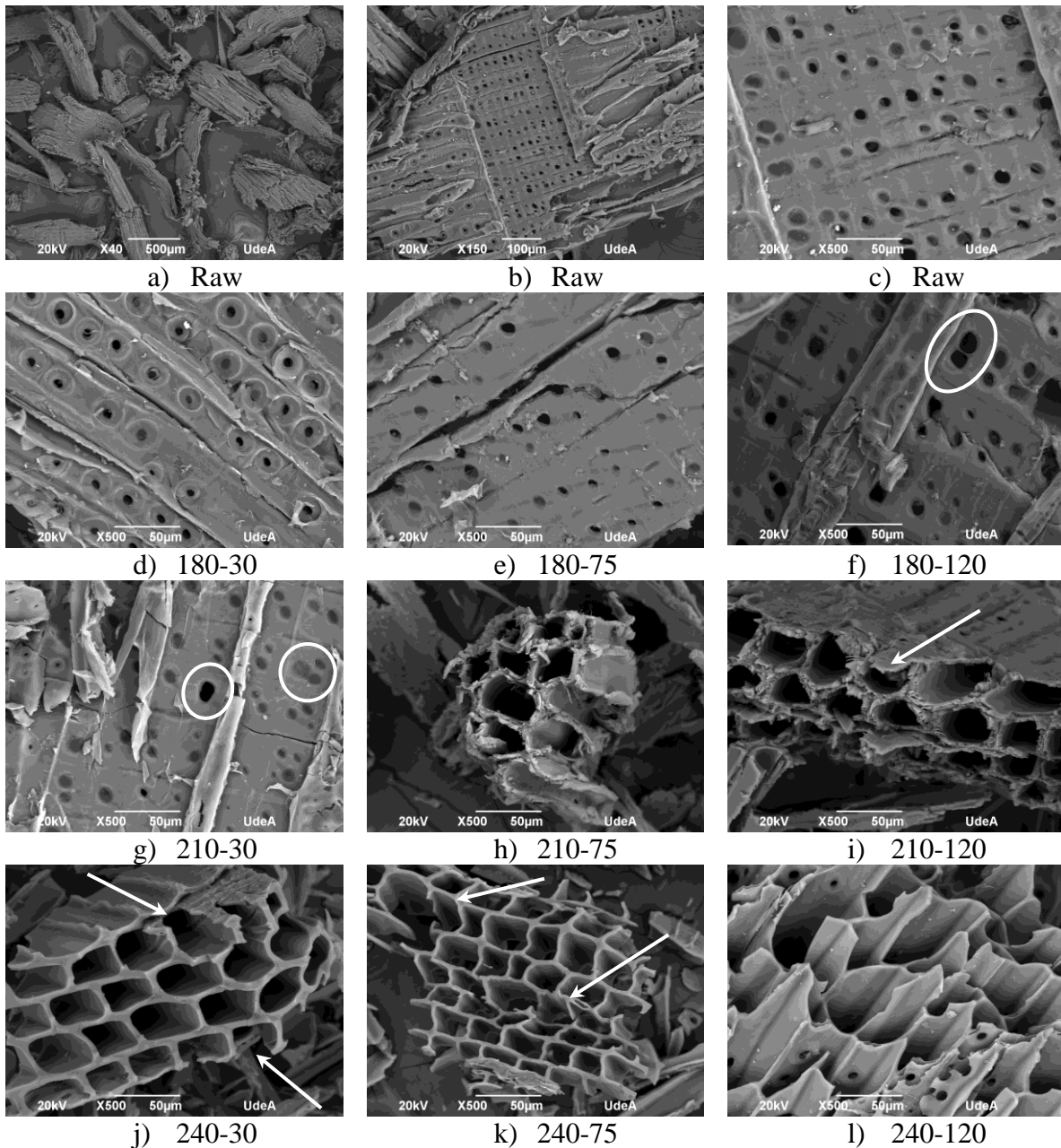


Figure 3.4. SEM images of raw and torrefied patula pine.

When the torrefaction severity reaches the 210 °C during 75 minutes and more severe conditions, the changes in morphology of the treated material start to be more evident. For torrefied pine at 210 °C during 75 and 120 minutes, cell walls exhibit structures with bigger and some destroyed pores regarding raw material due to the higher volatile matter released during torrefaction process. Likewise, pores of material torrefied during 120 minutes have suffered plastic deformation in the process leading to a collapse of the cell wall (see bold

arrows) due to secondary reactions that occur in the process. Furthermore, this torrefaction temperature is higher than the glass temperature of the hemicellulose and lignin which leads to softening of the cell wall of the material [47]. As a consequence of the collapse of the porous structure, the specific surface area of the material decreases; this is in agreement with the results obtained in relation to the surface area (section 3.3.4). Despite these structural changes, torrefied pine still shows a fibrous nature in the cell walls, which correspond to the presence of holocellulose after torrefaction process as described in section 3.3.2. When torrefaction temperature increases up to 240 °C, treated material has a more defined structure due to partial oxidation reactions that lead to a material rich in lignin. The fibrous nature of cell walls disappears implying the complete thermal degradation of hemicellulose and cellulose which agrees with the TGA analysis (section 3.3.2.). Since this torrefaction temperature is the most severe, porosity is enhanced, and pore destruction becomes more evident as seen in Figure 3.4.

The increase in porosity of torrefied material can be related to an enhancement in its thermal behavior and its grindability. The thermal behavior improves due to the higher porosity of the material; which leads to obtain higher heat and mass transfer areas in solid-gas reactions associated with pyrolysis, gasification, or combustion processes. Additionally, the structure of a porous material is more fragile implying less energy power consumption by grinding. Therefore, torrefaction process under an oxidizing atmosphere is a feasible process to be conducted to improve the physicochemical properties of wood biomass.

Conclusions

Changes in chemical structure and morphology of patula pine torrefied under an oxidizing atmosphere were studied. Wood biomass composition is affected by temperature and residence time. Volatile matter content tends to decrease when torrefaction is conducted at low temperatures. However, for the most severe temperature condition (i.e. 240 °C) it increases with residence time; since oxidation reactions on biomass surface are favored by the duration of torrefaction process. Carbon content of torrefied pine also increases with torrefaction severity. Due to severe thermal degradation of the wood constituents at the highest temperature (240 °C), it can be stated that biomass was subjected to partial combustion instead to a torrefaction process. Carbon contents for this torrefaction temperature reach values around 70%. This result agrees with the TGA analysis where no

devolatilization of hemicellulose and cellulose is observed. For low-temperature conditions (180 and 210 °C), the wood constituent that is mainly decomposed in the presence of oxygen is the cellulose. Moreover, the remaining cellulose in torrefied biomass suffers structural changes associated with depolymerization reactions. As a result, torrefied biomass at these temperature conditions exhibits higher thermal stability. Nevertheless, the thermal degradation of cellulose during torrefaction process may affect the behavior of the pretreated material if it is used as feedstock in a thermochemical process such as pyrolysis. It is expected that bio-oil obtained from pyrolysis of torrefied pine under the oxidizing atmosphere has lower levoglucosan and higher acetic acid contents.

Torrefaction under the oxidizing atmosphere upgrade wood biomass properties as solid biofuel due to the increase of C–O–C and C=C bonds in its chemical structure. These linkages can release higher energy than others in pine structure, which results in an increase in the heating value of the torrefied material. Likewise, torrefaction at low temperatures enhances the porosity of the material which improves its reactivity. At higher temperatures (240 °C), pore structure is destroyed, and material has char-like properties caused by the greater oxidation reactions that occur in the process. This behavior may also improve the grindability behavior of the pretreated material. According to the final application of the solid material, torrefaction under the oxidizing atmosphere may be a suitable process to upgrade wood biomass properties as feedstock.

Acknowledgements

The authors acknowledge Universidad de Antioquia for the financial support of this research through Projects “Estrategias de integración de la madera plantada en Colombia en conceptos de biorrefinería termoquímica: Análisis termodinámico y caracterización de bioproductos – PRG 2014-1016” and “Sostenibilidad 2015-2016”, and through the “Estudiante instructor” program.

References

- [1] Y. A. Lenis, A. F. Agudelo, and J. F. Pérez, “Analysis of statistical repeatability of a fixed bed downdraft biomass gasification facility,” *Appl. Therm. Eng.*, vol. 51, pp. 1006–1016, 2013.

- [2] R. H. H. Ibrahim, L. I. Darvell, J. M. Jones, and A. Williams, "Physicochemical characterisation of torrefied biomass," *J. Anal. Appl. Pyrolysis*, vol. 103, pp. 21–30, 2013.
- [3] T. G. Bridgeman, J. M. Jones, a. Williams, and D. J. Waldron, "An investigation of the grindability of two torrefied energy crops," *Fuel*, vol. 89, no. 12, pp. 3911–3918, 2010.
- [4] M. Phanphanich and S. Mani, "Impact of torrefaction on the grindability and fuel characteristics of forest biomass," *Bioresour. Technol.*, vol. 102, no. 2, pp. 1246–1253, 2011.
- [5] K. M. Lu, W. J. Lee, W. H. Chen, S. H. Liu, and T. C. Lin, "Torrefaction and low temperature carbonization of oil palm fiber and eucalyptus in nitrogen and air atmospheres," *Bioresour. Technol.*, vol. 123, pp. 98–105, 2012.
- [6] G. Xue, M. Kwapinska, W. Kwapinski, K. M. Czajka, J. Kennedy, and J. J. Leahy, "Impact of torrefaction on properties of *Miscanthus × giganteus* relevant to gasification," *Fuel*, vol. 121, pp. 189–197, 2014.
- [7] B. Arias, C. Pevida, J. Feroso, M. G. Plaza, F. Rubiera, and J. J. Pis, "Influence of torrefaction on the grindability and reactivity of woody biomass," *Fuel Process. Technol.*, vol. 89, no. 2, pp. 169–175, 2008.
- [8] M. Strandberg, I. Olofsson, L. Pommer, S. Wiklund-Lindström, K. Åberg, and A. Nordin, "Effects of temperature and residence time on continuous torrefaction of spruce wood," *Fuel Process. Technol.*, vol. 134, pp. 387–398, 2015.
- [9] L. D. Mafu, H. W. J. P. Neomagus, R. C. Everson, M. Carrier, C. A. Strydom, and J. R. Bunt, "Structural and chemical modifications of typical South African biomasses during torrefaction," *Bioresour. Technol.*, vol. 202, pp. 192–197, 2016.
- [10] L. E. Arteaga-Pérez, C. Segura, D. Espinoza, L. R. Radovic, and R. Jiménez, "Torrefaction of *Pinus radiata* and *Eucalyptus globulus*: A combined experimental and modeling approach to process synthesis," *Energy Sustain. Dev.*, vol. 29, pp. 13–23, 2015.
- [11] V. Repellin, A. Govin, M. Rolland, and R. Guyonnet, "Energy requirement for fine grinding of torrefied wood," *Biomass and Bioenergy*, vol. 34, no. 7, pp. 923–930, 2010.
- [12] S. Saadon, Y. Uemura, and N. Mansor, "Torrefaction in the Presence of Oxygen and Carbon Dioxide: The Effect on Yield of Oil Palm Kernel Shell," *Procedia Chem.*, vol. 9, pp. 194–201, 2014.

- [13] W. H. Chen, K. M. Lu, S. H. Liu, C. M. Tsai, W. J. Lee, and T. C. Lin, "Biomass torrefaction characteristics in inert and oxidative atmospheres at various superficial velocities," *Bioresour. Technol.*, vol. 146, no. x, pp. 152–160, 2013.
- [14] P. Rousset, L. MacEdo, J. M. Commandré, and a. Moreira, "Biomass torrefaction under different oxygen concentrations and its effect on the composition of the solid by-product," *J. Anal. Appl. Pyrolysis*, vol. 96, pp. 86–91, 2012.
- [15] Y. Joshi, M. Di Marcello, E. Krishnamurthy, and W. De Jong, "Packed-Bed Torrefaction of Bagasse under Inert and Oxygenated Atmospheres," vol. 29, 2015.
- [16] Y. Uemura, W. Omar, N. A. Othman, S. Yusup, and T. Tsutsui, "Torrefaction of oil palm EFB in the presence of oxygen," *Fuel*, vol. 103, pp. 156–160, 2013.
- [17] W. H. Chen, K. M. Lu, W. J. Lee, S. H. Liu, and T. C. Lin, "Non-oxidative and oxidative torrefaction characterization and SEM observations of fibrous and ligneous biomass," *Appl. Energy*, vol. 114, pp. 104–113, 2014.
- [18] B. M. Esteves, I. J. Domingos, and H. M. Pereira, "Pine wood modification by heat treatment in air," *BioResources*, vol. 3, no. 1, pp. 142–154, 2008.
- [19] C. Wang, J. Peng, H. Li, X. T. Bi, R. Legros, C. J. Lim, and S. Sokhansanj, "Oxidative torrefaction of biomass residues and densification of torrefied sawdust to pellets," *Bioresour. Technol.*, vol. 127, pp. 318–325, 2013.
- [20] S. J. Hill, W. J. Grigsby, and P. W. Hall, "Chemical and cellulose crystallite changes in *Pinus radiata* during torrefaction," *Biomass and Bioenergy*, vol. 56, pp. 92–98, 2013.
- [21] J. G. Pohlmann, E. Osorio, A. C. F. Vilela, M. A. Diez, and A. G. Borrego, "Integrating physicochemical information to follow the transformations of biomass upon torrefaction and low-temperature carbonization," *Fuel*, vol. 131, pp. 17–27, 2014.
- [22] J. F. Pérez and L. F. Osorio, *Biomasa forestal como alternativa energética: Análisis silvicultural, técnico y financiero de proyectos*. Medellín: Universidad de Antioquia, 2014.
- [23] J. F. Pérez, A. Melgar, and P. N. Benjumea, "Effect of operating and design parameters on the gasification/combustion process of waste biomass in fixed bed downdraft reactors: An experimental study," *Fuel*, vol. 96, pp. 487–496, 2012.

- [24] Y. A. Lenis and J. F. Pérez, "Gasification of Sawdust and Wood Chips in a Fixed Bed under Autothermal and Stable Conditions," *Energy Sources, Part A Recover. Util. Environ. Eff.*, vol. 36, no. 23, pp. 2555–2565, 2014.
- [25] D. Medic, M. Darr, A. Shah, B. Potter, and J. Zimmerman, "Effects of torrefaction process parameters on biomass feedstock upgrading," *Fuel*, vol. 91, no. 1, pp. 147–154, 2012.
- [26] ASTM, "D5373-08 Standard Test Methods for Instrumental Determination of Carbon, Hydrogen, and Nitrogen in Laboratory Samples of Coal," *Annu. B. ASTM Stand.*, vol. 5, no. October 2002, pp. 1–9, 2012.
- [27] R. Barrera Zapata, J. F. Pérez Bayer, and C. Salazar Jiménez, "Colombian coals: classification and thermochemical characterization for energy applications," *Rev. ION*, vol. 27, no. 2, pp. 43–54, 2014.
- [28] P. Ghetti, "DTG combustion behaviour of coal. Correlations with proximate and ultimate analysis data," *Fuel*, vol. 65, no. 5, pp. 636–639, 1986.
- [29] W. H. Chen and P. C. Kuo, "A study on torrefaction of various biomass materials and its impact on lignocellulosic structure simulated by a thermogravimetry," *Energy*, vol. 35, no. 6, pp. 2580–2586, 2010.
- [30] M. R. Pelaez-Samaniego, V. Yadama, M. Garcia-Perez, E. Lowell, and A. G. McDonald, "Effect of temperature during wood torrefaction on the formation of lignin liquid intermediates," *J. Anal. Appl. Pyrolysis*, vol. 109, pp. 222–233, 2014.
- [31] J. Park, J. Meng, K. H. Lim, O. J. Rojas, and S. Park, "Transformation of lignocellulosic biomass during torrefaction," *J. Anal. Appl. Pyrolysis*, vol. 100, pp. 199–206, 2013.
- [32] J. J. Lu and W. H. Chen, "Product yields and characteristics of corncob waste under various torrefaction atmospheres," *Energies*, vol. 7, no. 1, pp. 13–27, 2014.
- [33] D. Eseltine, S. S. Thanapal, K. Annamalai, and D. Ranjan, "Torrefaction of woody biomass (Juniper and Mesquite) using inert and non-inert gases," *Fuel*, vol. 113, pp. 379–388, 2013.
- [34] J. Klinger, E. Bar-Ziv, and D. Shonnard, "Unified kinetic model for torrefaction–pyrolysis," *Fuel Process. Technol.*, vol. 138, pp. 175–183, 2015.

- [35] S. Ramos C., J. F. Pérez, M. R. Pelaez-Samaniego, R. Barrera, and M. Garcia-Perez, "Effect of torrefaction temperature on properties of Patula Pine," *Maderas. Cienc. y Tecnol.*, 2017.
- [36] Z. Yang, M. Sarkar, A. Kumar, J. S. Tumuluru, and R. L. Huhnke, "Effects of torrefaction and densification on switchgrass pyrolysis products," *Bioresour. Technol.*, vol. 174, pp. 266–273, 2014.
- [37] S. Zhang, Q. Dong, L. Zhang, and Y. Xiong, "Effects of water washing and torrefaction on the pyrolysis behavior and kinetics of rice husk through TGA and Py-GC/MS," *Bioresour. Technol.*, no. 199, pp. 352–361, 2016.
- [38] A. Zheng, Z. Zhao, S. Chang, Z. Huang, X. Wang, F. He, and H. Li, "Comparison of the effect of wet and dry torrefaction on chemical structure and pyrolysis behavior of corncobs," *Bioresour. Technol.*, vol. 176, pp. 15–22, 2015.
- [39] R. M. Silverstein, F. X. Webster, D. J. Kiemle, and D. L. Bryce, *Spectrometric identification of organic compounds*. John Wiley & Sons, 2014.
- [40] T. Singh, A. P. Singh, I. Hussain, and P. Hall, "Chemical characterisation and durability assessment of torrefied radiata pine (*Pinus radiata*) wood chips," *Int. Biodeterior. Biodegrad.*, vol. 85, pp. 347–353, 2013.
- [41] M. R. Pelaez-Samaniego, V. Yadama, E. Lowell, and R. Espinoza-Herrera, "A review of wood thermal pretreatments to improve wood composite properties," *Wood Sci. Technol.*, vol. 47, no. 6, pp. 1285–1319, 2013.
- [42] B. Esteves, A. Velez Marques, I. Domingos, and H. Pereira, "Chemical changes of heat treated pine and eucalypt wood monitored by FTIR," *Maderas. Cienc. y Tecnol.*, vol. 15, no. ahead, pp. 245–258, 2013.
- [43] L. Shang, J. Ahrenfeldt, J. K. Holm, A. R. Sanadi, S. Barsberg, T. Thomsen, W. Stelte, and U. B. Henriksen, "Changes of chemical and mechanical behavior of torrefied wheat straw," *Biomass and Bioenergy*, vol. 40, pp. 63–70, 2012.
- [44] J. W. Lee, Y. H. Kim, S. M. Lee, and H. W. Lee, "Optimizing the torrefaction of mixed softwood by response surface methodology for biomass upgrading to high energy density," *Bioresour. Technol.*, vol. 116, pp. 471–476, 2012.

- [45] S. W. Park, C. H. Jang, K. R. Baek, and J. K. Yang, "Torrefaction and low-temperature carbonization of woody biomass: Evaluation of fuel characteristics of the products," *Energy*, vol. 45, no. 1, pp. 676–685, 2012.
- [46] Q. Chen, J. S. Zhou, B. J. Liu, Q. F. Mei, and Z. Y. Luo, "Influence of torrefaction pretreatment on biomass gasification technology," *Chinese Sci. Bull.*, vol. 56, no. 14, pp. 1449–1456, 2011.
- [47] Y. Uemura, S. Saadon, N. Osman, N. Mansor, and K. Tanoue, "Torrefaction of oil palm kernel shell in the presence of oxygen and carbon dioxide," *Fuel*, vol. 144, pp. 171–179, 2015.

Chapter 4: Effect of torrefied wood biomass under an oxidizing atmosphere on downdraft gasification process

Sergio Ramos-Carmona, Juan F. Pérez

Abstract

The performance of downdraft gasification process under autothermal conditions using torrefied biomass under an oxidizing atmosphere is studied in this work. An extended model in thermochemical equilibrium is used to evaluate the effect of torrefaction conditions, fuel/air equivalence ratio, and biochar production as a byproduct on producer gas composition, reaction temperature, cold gas efficiency, and the quality of the producer gas for internal combustion engine applications. The model was validated with a global relative error of 8.5% without considering methane concentration. Gasification of torrefied wood biomass at 180, 210, and 240 °C during 30, 75, and 120 minutes was simulated with the model. Biochar production affects the gasification performance due to the modification in the actual fuel/air ratio which leads to that the process tends to combustion regimes. Increasing fuel/air equivalence ratio allows to obtaining higher cold gas efficiencies (up to 80%) and improve the quality of the syngas for engine applications (up to 2.5 MJ/kg). Regarding torrefaction conditions, an increase in process efficiency (from 77 to 82%) and quality of the producer gas (from 2.2 to 2.5 MJ/kg) can be achieved. This result is related to the increase of the autothermal zones in the gasification process and feedstock heating value with torrefaction severity (biomass with lower O/C and H/C ratios). Therefore, torrefaction under the oxidizing atmosphere to upgrade biomass prior its gasification is a suitable process to improve process performance, especially for internal combustion engine applications of the producer gas. Likewise, considering the biochar production during gasification in the extended model is a useful tool to simulate with more accuracy this thermochemical process.

Keywords: Downdraft gasification, thermochemical equilibrium, torrefaction, oxidizing atmosphere, Patula pine wood.

4.1. Introduction

Biomass is a renewable energy with a great potential to substitute partially and to reduce the fossil fuels dependence, mainly due to its high and decentralized availability, and versatility [1]. From biomass, it can be obtained solid, liquid, and gaseous products useful to further thermochemical or industrial processes [2]. Moreover, the use of biomass as energy source aids to mitigate environmental issues by pollutant emissions and to contribute to the goals proposed in the climate change conference COP 21 [3]. However, biomass as feedstock has several disadvantages such as high moisture content, low energy content, and hydrophilic nature resulting in high cost of transportation and storage [4].

Several strategies have been studied in order to upgrade biomass properties such as torrefaction. Torrefaction is considered as a mild pyrolysis process (200–300 °C) conducted under inert atmospheres during times less than 1h commonly [5]–[7]. A torrefied biomass exhibits better properties than the raw material due to the reduction in the moisture content and O/C ratio by thermal decomposition of hemicellulose [5], [8], [9]. Thereby, a pretreated biomass has higher heating value, better grindability behavior which reduces power consumption by grinding, and it acquires hydrophobic nature [10], [11].

The supply of an inert gas during torrefaction process increases the operation costs of the process. An alternative way to reduce the production cost is using air as carrier gas to conduct an oxidative torrefaction process [12]. The effect of changing the torrefaction atmosphere on biomass properties has been studied widely [13]–[16]. It has been reported that torrefaction under an oxidizing atmosphere favors oxidation reactions on the biomass surface and of the volatile matter released during the process [16]. The main constituent thermally degraded during the pretreatment is the cellulose instead of hemicellulose [13]. Additionally, authors stated that the change of atmosphere is suitable for torrefaction of lignocellulosic biomass since its cell wall structure is relatively insensitive to the oxidizing environment [12], [15].

Torrefied biomass is often used in co-firing with coal and gasification applications. For co-firing conditions, several studies reported that the electrical efficiency decreases when increasing torrefaction temperature or biomass substitution ratio. Moreover, severe torrefaction temperatures were not suitable since the power consumption saved during grinding does not compensate the heat consumed during the pretreatment [17]. On the other

hand, NO_x and SO_x emissions diminish when torrefied biomass is co-fired with coal, due to the lower sulfur and nitrogen contents of biomass. Likewise, SO₂ emissions decrease as a result of sulfur in ash due to this inert matter is mainly constituted by calcium, magnesium, and potassium [18].

Gasification is a process that converts a solid feedstock into a gaseous fuel through its partial oxidation with a gasifying agent; e.g. air, pure oxygen, water vapor, or mixtures [1]. The producer gas can be burned in turbines or internal combustion engines for power generation, or used for the production of value-added chemicals [19]. The process using torrefied biomass as feedstock has been studied for all gasification technologies. For entrained flow gasifiers, torrefied biomass tended to produce more syngas with higher H₂ and CO concentration; therefore higher gasification efficiencies were achieved [7], [20], [21]. Also, depending on the torrefaction severity, higher carbon conversion efficiencies were reached [22]. Higher gas yield, gasification temperatures, producer gas heating value, and overall efficiencies were obtained in fluidized bed reactors [4], [6], [23]. Furthermore, lower tars yield and lower exergy efficiencies were achieved with this technology if the volatiles released during torrefaction are not exploited [4], [6].

For fixed bed gasifiers, authors stated that torrefied biomass also led to higher syngas yield, H₂ and CO concentrations, cold gas efficiencies, and lower tars yield regarding the raw material [24]–[26]. Nevertheless, these findings were obtained under non-autothermal conditions because the reaction temperature was fixed either in the experimental [26] or simulated [24], [25] studies. For an autothermal process, the reaction temperature is affected by the feedstock (heating value) and the fuel/air equivalence ratio [27].

The aim of this work is to study the effect of torrefied biomass under an oxidizing atmosphere on downdraft gasification performance under autothermal conditions. An extended model in thermochemical equilibrium is used to evaluate the effect of changes in chemical composition (ultimate analysis) of biomass subjected to different torrefaction conditions, fuel/air equivalence ratio, and biochar production as a by-product of the gasification process. Biochar production is a measure of the fraction of initial biomass feed into the gasifier that does not become into syngas; which makes the gasification process inefficient [1]. The response variables analyzed are the syngas composition, reaction temperature, and other thermodynamic parameters of the gasification process such as

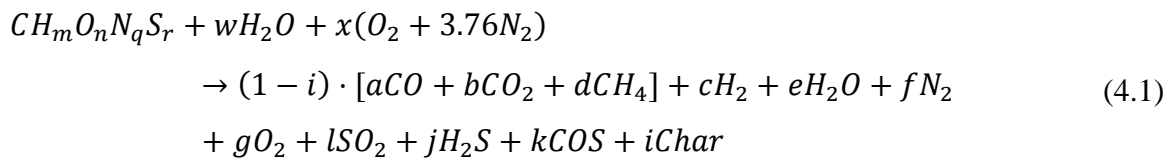
producer gas heating value and cold gas efficiency are studied. Additionally, quality of producer gas to fuel internal combustion engines is also evaluated by means of the engine fuel quality.

4.2. Materials and methods

4.2.1. Model description

The model used in this work is an extended version of the approach presented by Melgar et al. [27]. It combines chemical and thermodynamic equilibrium of the global gasification reaction. This model is a helpful tool to predict producer gas (PG) composition and the reaction temperature of the gasification process. Furthermore, from PG composition, it is possible to determine other important parameters such as lower heating value (LHV_{pg}), cold gas efficiency (CGE), and engine fuel quality (EFQ) [19], [27]. These parameters relate the quality as a fuel of the PG for direct combustion or for spark ignition engines applications. Therefore, the model approach is useful to study the gasification performance in function of biomass composition, biomass moisture content, and fuel/air equivalence ratio (Fr) [27].

The modifications carried out to the thermochemical equilibrium model take into account other gasification products by sulfur present in biomass, and a remaining solid fraction at the end of the gasification process (i.e. biochar). PG is modeled as an ideal gas mixture, and reactor operates at atmospheric pressure [27]. Therefore, the new global reaction of the gasification process used in the extended model is:



The gasification products added to the model associated with biomass sulfur are H₂S and COS. According to Álvarez-Rodríguez and Clemente-Jul [28], these are the main product from the thermochemical conversion of sulfur in lean-oxygen environments (i.e. gasification regimes). Since two compounds are introduced into the model, two new reaction is equilibrium are required. Martínez et al. [29] used these reactions in their work about the syngas production from volatiles released in waste tire pyrolysis (Eq. 4.5 and

4.6). Additionally, it is considered the biochar (modeled as pure carbon) production (Eq. 4.7), which is a byproduct of a real gasification process [30], [31]. Table 4.1 shows the main model equations (4.2-4.7).

Table 4.1. Equations and equilibrium reaction of the thermodynamic model

Thermochemical equilibrium model	Equation
$x = \frac{1}{F_r F_{stq,bms}}$	(4.2)
$C + 2H_2 \leftrightarrow CH_4$	(4.3)
$\therefore K_1 = \frac{(P_{CH_4}/P_0)}{(P_{H_2}/P_0)^2} = \frac{dn_T}{c^2}$	(4.4)
$CO + H_2O \leftrightarrow CO_2 + H_2$	(4.5)
$\therefore K_2 = \frac{(P_{CO_2}/P_0)(P_{H_2}/P_0)}{(P_{CO}/P_0)(P_{H_2O}/P_0)} = \frac{bc}{ae}$	(4.5)
$CO + H_2S \leftrightarrow COS + H_2$	(4.6)
$\therefore K_3 = \frac{(P_{COS}/P_0)(P_{H_2}/P_0)}{(P_{CO}/P_0)(P_{H_2S}/P_0)} = \frac{kc}{aj}$	(4.6)
$COS + 2CO_2 \leftrightarrow 3CO + SO_2$	(4.7)
$\therefore K_4 = \frac{(P_{CO}/P_0)(P_{SO_2}/P_0)}{(P_{COS}/P_0)(P_{CO_2}/P_0)} = \frac{al}{kb}$	(4.7)
$i = \frac{\text{unreacted carbon moles}}{\text{carbon moles in biomass}} \quad \therefore 0 \leq i < 1$	(4.7)

From the ultimate analysis of biomass and the moisture content is calculated the substitution formula of biomass ($CH_mO_nN_qS_r$) and the molar quantity of water [27]. With this formula, fuel/air ratio under stoichiometric conditions is determined. Thereby, from this parameter and fuel/air equivalence ratio, the real air molar quantity is calculated (Eq. 4.2). Moreover, the enthalpy of reactants is estimated.

An iterative process in function of the reaction temperature is conducted. With an initial reaction temperature, PG composition is determined by solving the nonlinear system equations using the Newton-Raphson method. Subsequently, the reaction temperature is calculated from the energy balance between reactants (biomass, moisture, and air) and

products (PG, biochar). The calculated temperature is used in the next iterative step until chemical and thermal equilibrium are reached. A detailed procedure for solving the model and auxiliary equations are reported by Pérez et al. [19].

4.2.2. Model validation

The purpose of the present study is to evaluate the gasification performance using torrefied biomass as feedstock under autothermal conditions. Therefore, experimental data reported in the master thesis by Bibens [32] have been used to validate the accuracy of the extended model under downdraft gasification conditions using torrefied wood biomass as biofuel. Bibens [32] evaluated the effect of torrefied pine chips on gasification performance by measuring yields, efficiency, and tar production during the process. The gasification facility used in his work is a two-stage downdraft fixed bed gasifier. Pine torrefaction was conducted under an inert atmosphere in a batch rotary kiln at different temperature and residence time conditions. Table 4.2 shows the different composition and heating value for raw and torrefied biomass evaluated by Bibens. Torrefaction conditions are coded as temperature-time (e.g. 250-30 means a torrefaction temperature of 250 °C for 30 minutes of residence time). Moreover, gasification parameters such as fuel/air equivalence ratio and char yield are shown. These values were used as input data in the model.

Table 4.2. Experimental data used for model validation, adapted from [32].

Sample	Ultimate analysis [wt. % daf ^a]				Moisture [wt. %]	LHV _{bms} [kJ/kg]	Fr	Char yield [wt. %]
	C	H	N	O				
Raw	49.14	5.59	0.16	45.11	4.43	17470	3.13	1.02
Raw	49.14	5.59	0.16	45.11	9.35	17470	3.03	0.53
250-30	54.83	5.77	1.03	38.37	1.83	20960	2.94	0.30
250-60	55.23	5.94	0.81	38.02	2.15	21410	2.94	3.69
275-30	59.39	5.53	0.21	34.87	3.33	22660	2.70	0.30
275-60	60.78	5.60	0.23	33.39	3.08	23380	2.56	0.34
300-30	68.85	5.26	0.52	25.36	2.01	26670	2.78	3.71
300-60	73.04	5.06	0.29	21.61	1.18	28350	1.69	1.10

^adry ash free

Gasification runs carried out by Bibens were conducted controlling input parameters such as fuel/air equivalence ratio and gasification zone temperature at approximately 800 °C to maintain consistency [32]. The steady state of the process was considered when output PG temperature reached 400 °C. PG composition was determined by gas

chromatography, and biochar collection was conducted at two hours interval of operation. The detailed description of the experimental study is presented by Bibens [32].

4.2.3. Wood analyzed

Patula pine wood was selected due to its silvicultural potential in Colombian lands. This fast growing wood exhibits great characteristics such as high planted areas (3849 ha), high mean annual increment (MAI, 20 m³/ha/year), and low harvested time (13 years). Properties of pine as wood biofuel have been upgraded by means of torrefaction process under an oxidizing atmosphere (air) in a rotary kiln. Table 4.3 shows the different torrefaction conditions and its effect on the chemical composition and heating value of the pretreated material. Heating values of the different samples are estimates through the correlation reported by Friedl et al. [33] in function of ultimate analysis of biomass, sulfur in patula pine was not found. A detailed study of the effect of torrefaction under an oxidizing atmosphere on pine wood properties is found in chapters 2 and 3.

Table 4.3. Chemical composition and heating value of raw and torrefied patula pine

Sample	Ultimate analysis [wt. % daf ^a]				O/C	H/C	LHV _{bms} [MJ/kg]	F _{stq,bms} [kg _{bms} /kg _{air}]
	C	H	N	O				
Raw	55.70 (0.21)	7.14 (0.07)	0.19 (0.01)	36.97 (0.28)	0.664	0.128	16.85	0.180
180-300	55.15 (0.24)	7.20 (0.07)	0.15 (0.15)	37.50 (0.21)	0.680	0.131	15.94	0.194
180-750	55.40 (0.46)	6.96 (0.24)	0.00 (0.00)	37.64 (0.22)	0.679	0.126	16.30	0.192
180-120	56.45 (0.19)	6.60 (0.03)	0.48 (0.03)	36.47 (0.25)	0.646	0.117	17.12	0.184
210-300	56.91 (0.02)	6.74 (0.19)	0.44 (0.02)	35.91 (0.19)	0.631	0.118	17.25	0.181
210-750	58.15 (0.06)	6.59 (0.01)	0.22 (0.01)	35.04 (0.07)	0.603	0.113	17.76	0.176
210-120	57.68 (0.51)	6.51 (0.06)	0.00 (0.00)	35.81 (0.57)	0.621	0.113	17.19	0.185
240-300	76.03 (0.05)	3.75 (0.06)	0.35 (0.04)	19.87 (0.06)	0.261	0.049	23.90	0.133
240-750	72.58 (0.23)	2.49 (0.02)	0.02 (0.02)	24.91 (0.23)	0.343	0.034	21.08	0.159
240-120	71.17 (0.17)	2.65 (0.19)	0.08 (0.01)	26.10 (0.01)	0.367	0.037	21.16	0.158

*Values in parenthesis correspond to standard deviations

^adry ash free

As it can be seen, torrefaction process tends to increase carbon content while decrease hydrogen and oxygen contents. For 180-30 and 180-75 their chemical composition is similar to raw pine and changes are associated with the equipment variability used to conduct these analyses. For a temperature of 240 °C, the chemical composition of torrefied pine is similar to a biochar obtained by carbonization instead of a wood biomass as a consequence of the oxidation reactions that occur during the pretreatment [15]. The heating value of the pretreated material increases with torrefaction severity. Several authors have

reported similar results for torrefied biomass under inert and oxidizing atmospheres [12], [15], [34]. Changes in biomass composition are related to the thermal degradation of main wood constituents (cellulose and hemicellulose) during torrefaction process [9], [13].

4.3. Results and discussion

The model validation with experimental data, a sensitivity analysis of biochar production and fuel/air equivalence ratio, and the effect of torrefaction conditions on gasification performance is presented. The main parameters of the thermochemical process analyzed are PG composition and LHV, reaction temperature, CGE, and EFQ.

4.3.1. Model validation

Figure 4.1 shows a comparison between experimental data and model response variables. Results for PG composition, heating value, and CGE exhibit a good agreement between model and experimental data. Numerical results tend to overestimate CO concentration and underestimate CO₂ concentration slightly, while H₂ and CH₄ concentrations are also underestimated; therefore, due to the higher CO concentration estimated by the model, the LHV_{pg} is slightly overestimated.

The torrefaction conditions where the model does not show a good agreement are the most severe pretreatment conditions (i.e. torrefaction at 300 °C). The chemical composition of torrefied biomass at this temperature has higher carbon content (see Table 4.2). Thereby, it is expected that CO and CO₂ concentrations in the PG increase when torrefied biomass at 300 °C is used as feedstock. Nevertheless, Bibens [32] reported lower CO and CO₂ concentrations (15% and 4.12% in average, respectively) using the pretreated biomass as feedstock regarding the concentration obtained with the raw material (CO: 23.84% and CO₂: 10.73% in average). However, Yang et al. [35] reported experimental and simulated data for air gasification of char. They reported higher CO concentration with respect to H₂ for all gasification conditions. This behavior agrees with the results of the present model.

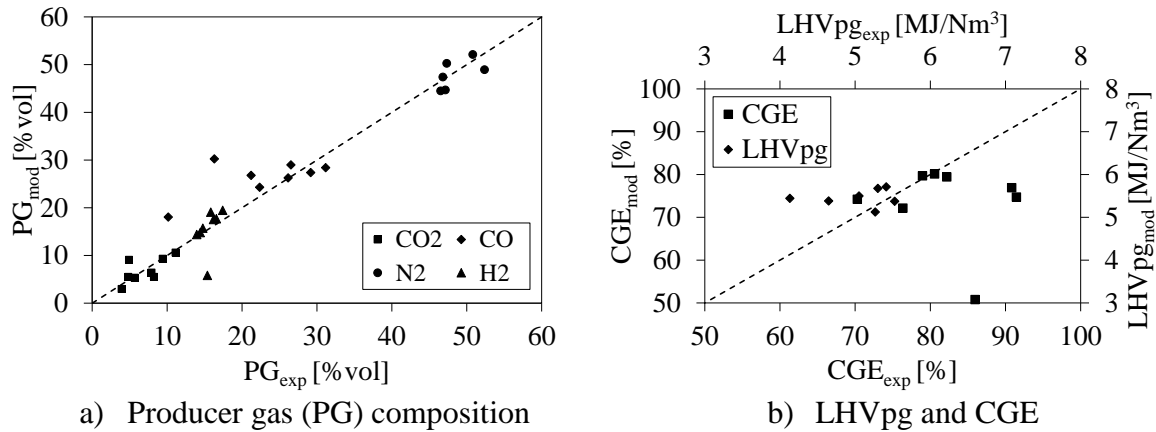


Figure 4.1. Model validation using torrefied wood gasification data reported by Bibens [32]

Table 4.4 shows the root mean square error (RMSE) and the relative error (RE) of the different response variables. Two columns (named “All conditions”) correspond to the errors including all torrefaction conditions (global average relative error of 24.8%, and without CH₄, 16%), and the other two (named “Except 300 °C”) correspond to the errors excluding the torrefaction conditions at 300 °C (global average relative error of 17.6%, and without CH₄, 8.5%). The experimental data associated with the gasification process using torrefied biomass at 300 °C increase both RMSE and RE for all variables. The exclusion of these torrefaction conditions leads to diminish the errors. Except for the CH₄, due to the lower concentration of this gaseous species. The accuracy of the response variables shows a good model behavior to simulate gasification process with torrefied biomass. Therefore, the model can be used as a useful tool to study the effect of torrefied wood biomass under an oxidizing atmosphere on the gasification performance considering the biochar production as byproduct.

Table 4.4. RMSE values for model validation.

Response variable	All conditions		Except 300°C	
	RMSE [\pm units]	RE [%]	RMSE [\pm units]	RE [%]
CO [% vol]	06.21	27.88	2.94	09.96
CO ₂ [% vol]	01.90	23.41	1.33	13.06
H ₂ [% vol]	03.71	15.24	1.78	09.45
N ₂ [% vol]	04.26	05.48	2.33	04.36
CH ₄ [% vol]	01.84	77.95	1.28	71.78
LHVpg [MJ/Nm ³]	00.67	12.29	0.41	07.12
CGE [%]	14.79	11.30	9.11	07.31

4.3.2. *Effect of biochar production and fuel/air equivalence ratio*

The model has been validated with good agreement for gasification process using torrefied biomass. Therefore, it can be used to study the effect of biochar production as a byproduct of the process and fuel/air equivalence ratio on gasification performance using torrefied wood as feedstock. Carbon conversion efficiencies may reach values from 70–95% and common fuel/air equivalence ratios for gasification processes are between 2 to 4 [19], [36], [37]. Therefore, factor “ i ” in the model was varied from 0 to 30% in order to consider the ideal thermodynamic behavior; i.e. when all carbon in biomass is converted to gas ($i=0$). The fuel/air equivalence ratio (Fr) was varied from 2 to 4.

Figure 4.2 shows the model results for the reaction temperature parametrized in function of torrefaction temperature conditions. Only results for 75 minutes as residence time are shown due to the similarities reached for the response variables with the different residence times analyzed (30, 75, and 120 minutes). The reaction temperature increases with increasing biochar production and decreasing fuel/air equivalence ratio. For these conditions, the actual fuel/air ratio of the process tends to diminish; thereby, the thermochemical process tends to combustion regimes leading to an increase in the reaction temperature. This behavior is associated with the model considerations, where all input air model reacts with the remaining biomass. From an experimental fixed bed gasification point of view, when the biochar production increases, the reaction temperature diminishes since the process occurs faster resulting in less time to favor the gasification stages [31]. For high fuel/air equivalence ratios and low biochar production, the model shows reaction temperatures around 400–600 °C; however, these temperatures do not allow achieving autothermal conditions in a real gasification facility. For lower temperatures, there is not enough energy in the reaction front to favor the endothermic stages of gasification process; such as drying, pyrolysis, and reduction [27], [38]. Therefore, a limit to describe autothermal process conditions must be established [38].

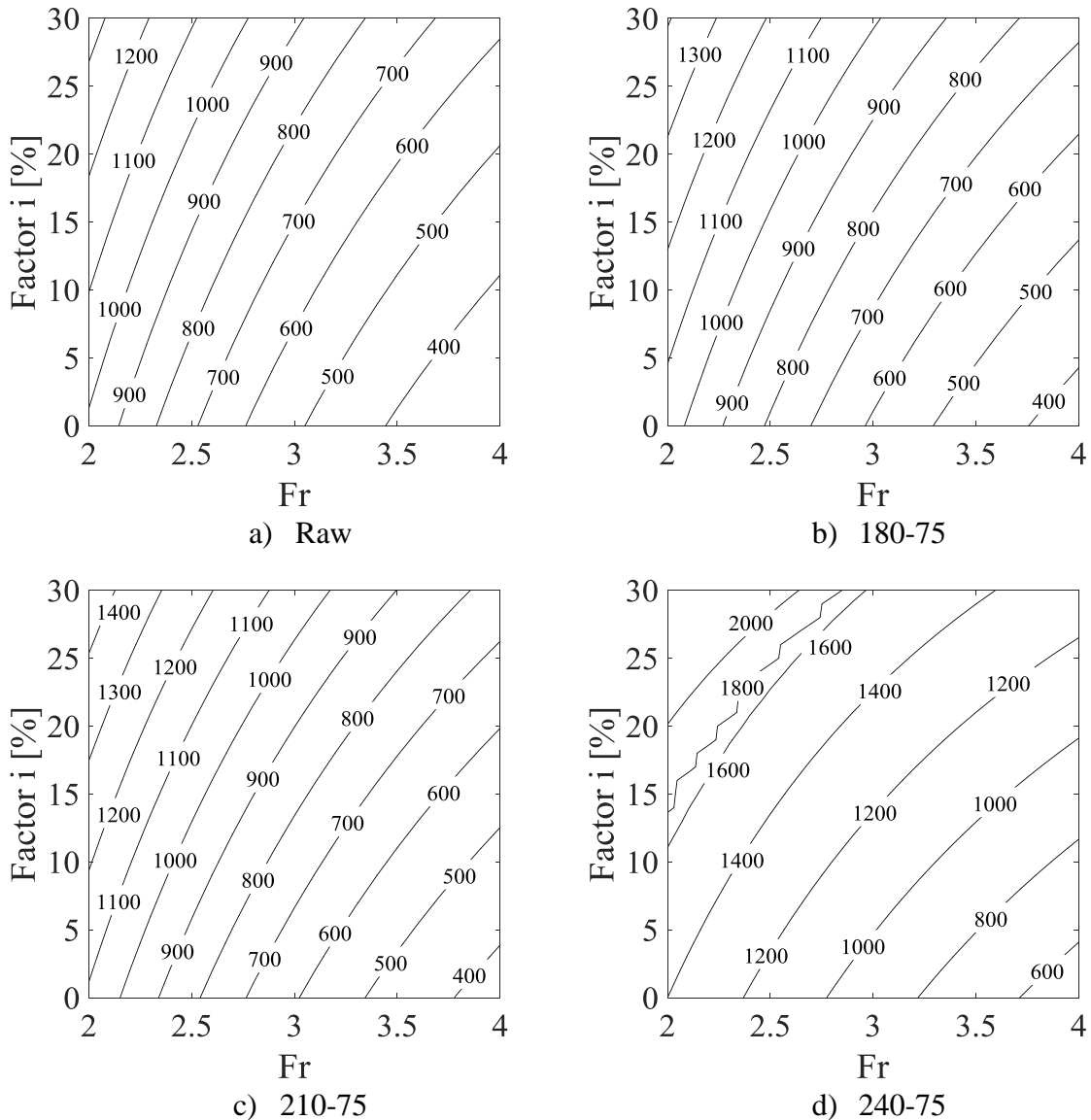


Figure 4.2. Reaction temperature of gasification [°C] for raw and torrefied pine in function of biochar production (Factor “*i*”) and Fr.

According to the lower temperatures reached for low biochar production and higher Fr (Figure 4.2), the Figure 4.3 shows the autothermal zones of the gasification process according to the reaction temperature calculated by the model. The limit for the autothermal zone is defined when the reaction temperature is equal to 650 °C [38]. Increasing torrefaction severity, temperature and/or residence time, the autothermal zone tends to become wider; i.e. the gasification process is stable at a greater Fr range and higher carbon conversion (or lower unreacted carbon fraction). This behavior is associated with the increase in the heating value of torrefied pine caused by the thermal degradation of wood

constituents [12]. Thereby, more energy is available in the gasification process resulting in a higher reaction temperature for a determined fuel/air equivalence ratio (Figure 4.2). These limits are taken into account to analyze the other response variables of the model considering the autothermal behavior.

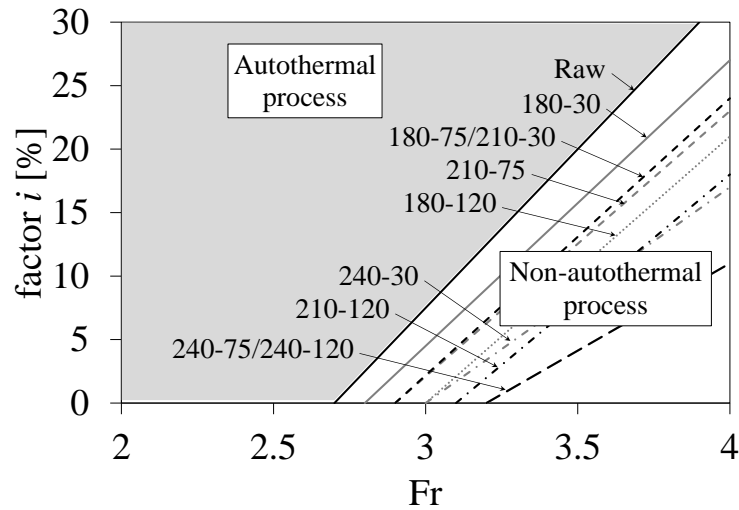


Figure 4.3. Autothermal zones in gasification process.

Figure 4.4 and Figure 4.5 show the CGE and the CO/CO₂ ratio in the producer gas in function of biochar production (factor “*i*”) and fuel/air equivalence ratio (Fr), respectively. The results are shown under autothermal conditions of the process for the different torrefaction conditions. CGE provides information about the energy conversion of biomass during gasification process; i.e. energy content of PG regarding the energy supplied by biomass [27].

For raw and torrefied pine, CGE decreases with increasing biochar production and decreasing the fuel/air equivalence ratio (Figure 4.4). As stated above, this behavior leads to the gasification process approaches combustion regimes; therefore, the production of CO₂ during the gasification increases (see Figure 4.5). Thereby, CO₂ and N₂ concentrations in the PG increase resulting in a reduction in its heating value. This finding agrees with the experimental results reported by Lenis et al. [31] in a fixed bed facility where a higher biochar production leads to decrease the CGE

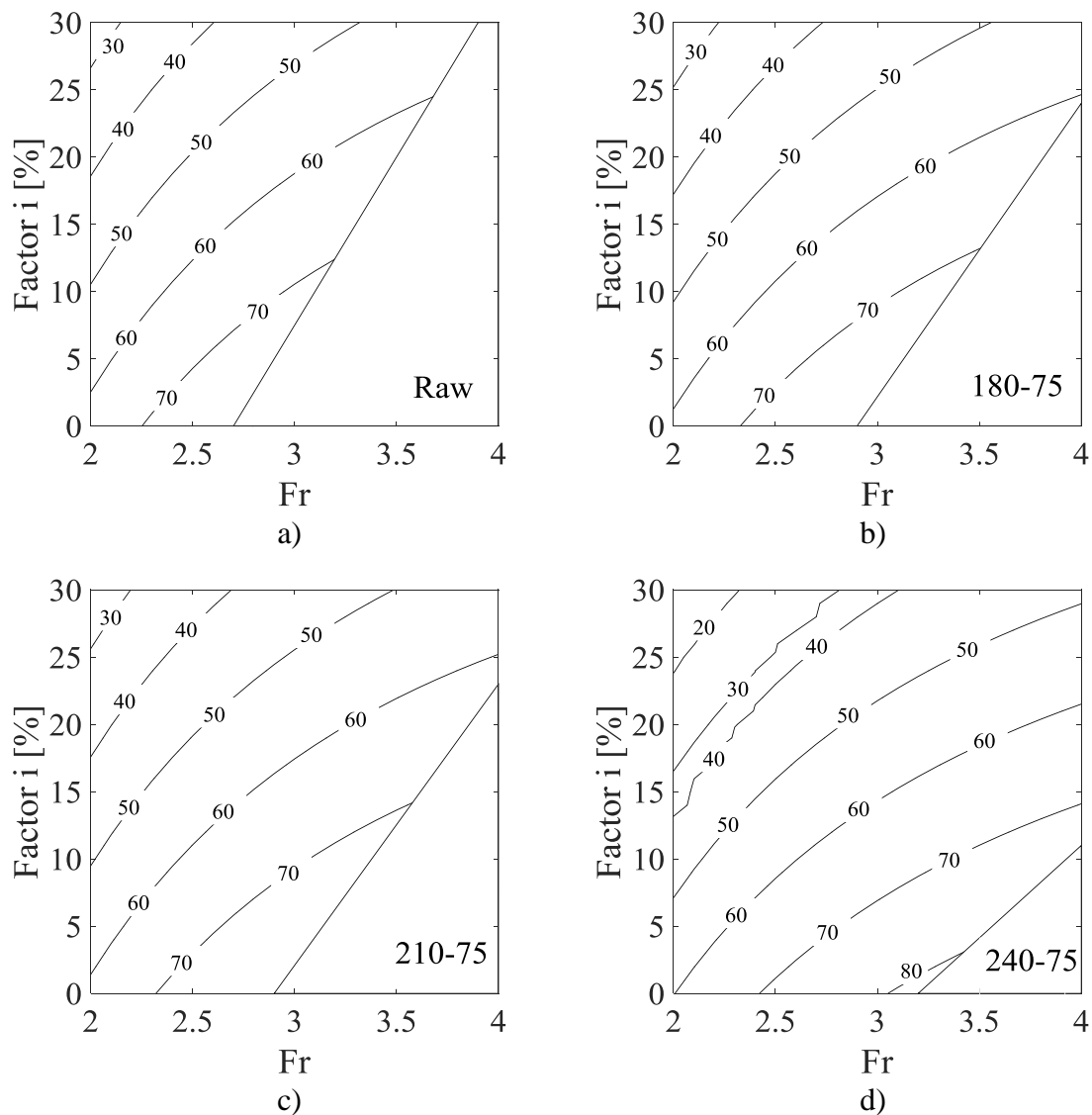


Figure 4.4. CGE [%] for raw and torrefied pine in function of biochar production (Factor “i”) and Fr.

Regarding Fr, CGE increases with Fr due to higher fuel-rich conditions are reached. A higher amount of carbon monoxide is produced as can be seen in Figure 4.5. Carbon monoxide is the gas with energy content more abundant in the PG (25–40%); thereby, the heating value of the PG increases with Fr resulting in higher CGE. Since torrefaction process increases the gasification autothermal zone; it is possible to achieve higher efficiencies regarding the raw material if the process is conducted at higher Fr. Tapasvi et al. [24] reported similar results for torrefied biomass under an inert atmosphere using a two-stage gasification model.

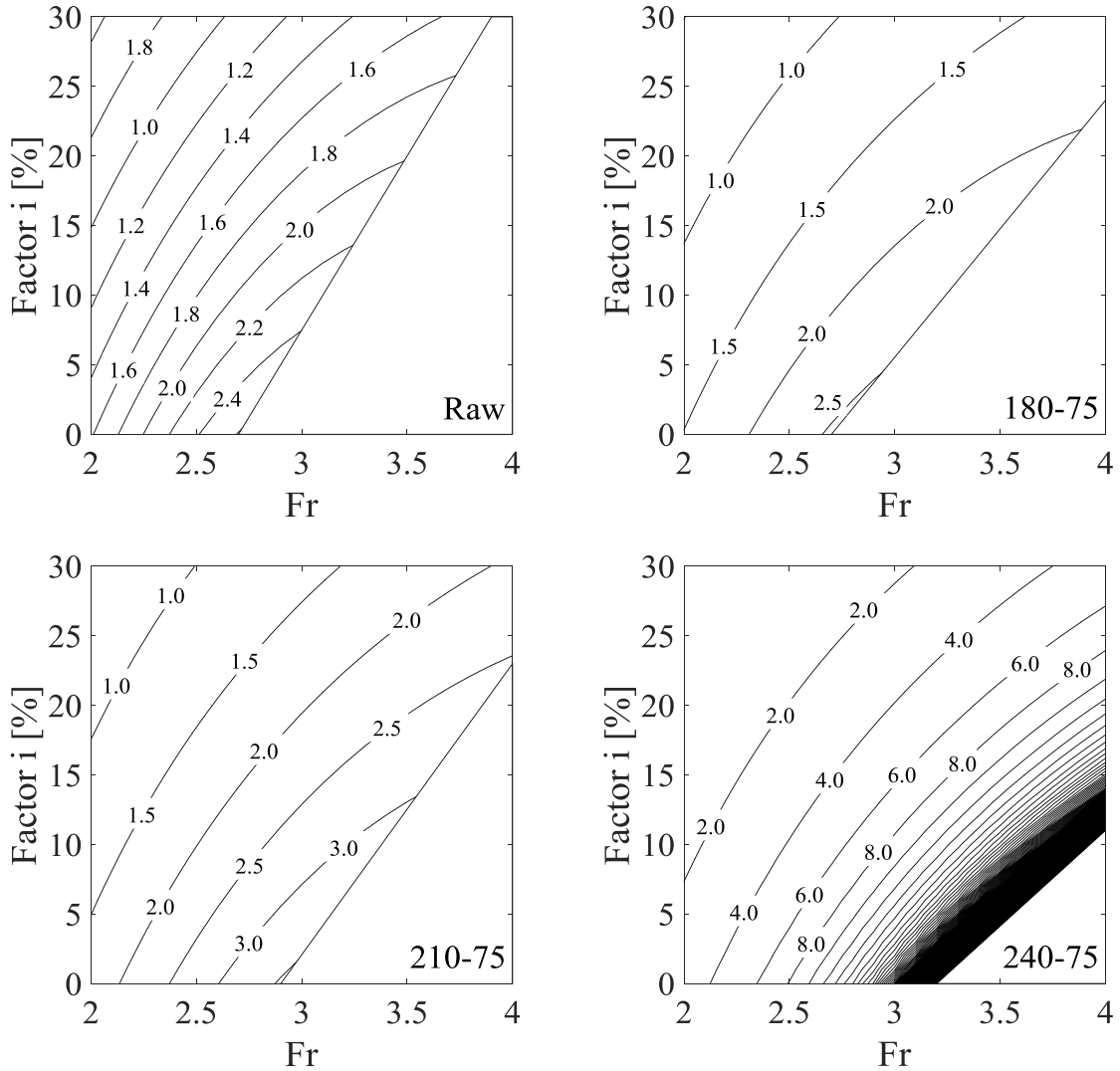


Figure 4.5. CO/CO₂ ratio for raw and torrefied pine in function of biochar production (Factor “*i*”) and Fr

As the torrefaction severity, the gasification process reaches autothermal conditions at higher Fr, but it is required to involve higher amount of biochar in the reaction, i.e., lower production of solid byproduct in the gasification process (lower factor “*i*”). Under this operating conditions, the CGE and reaction temperature increase due to the higher heating value of torrefied biomass (see Table 4.3). Therefore, the higher gasification temperature favors the auxiliary reactions (Eq. 4.3) to produce higher concentrations of gaseous fuels, which leads to higher efficiency under stable conditions.

4.3.3. *Effect of torrefaction under an oxidizing atmosphere*

In order to evaluate the effect of the torrefaction process under an oxidizing atmosphere on the gasification performance, the main thermodynamic parameters that characterize the process have been studied using the model. Thereby, the moisture content of raw and torrefied wood was not considered during simulations. With the aim to study the process thermodynamic limit, all simulations were conducted with no biochar production (i.e. factor “*i*” equals to zero) [6], and varying the fuel/air equivalence ratio from 2 to 3.2 [19], [36], [37]. For the torrefaction conditions, their response variables reach different Fr values; this is due to the differences in the autothermal zones for these materials as stated in the previous section. The analysis is conducted for all torrefaction conditions but for practical purposes, the torrefaction at 240 °C is not suitable due to the partial oxidation of biomass during the process.

4.3.3.1. *Reaction temperature*

Figure 4.6 shows the reaction temperature for raw and torrefied pine wood in function of Fr. For all samples, temperature decreases with increasing Fr in the gasification process; which is due to the lower amount of air in the global reaction. Therefore, if less air is involved in the gasification process, the energy released decreases resulting in a lower reaction temperature [27].

Regarding torrefaction process, reaction temperature depends on two biomass properties; namely heating value and fuel/air stoichiometric ratio. Higher torrefaction severity implies higher heating value; therefore, the energy released during gasification process is higher leading to an increase in the reaction temperature. However, the torrefied biomass with the highest heating value (240-30, see Table 4.3) does not reach the highest reaction temperature. The highest temperature condition is reached for a gasification process using torrefied pine at 240 °C for 75 minutes. This behavior is due to torrefied pine at 240-30 has higher carbon content, and lower fuel/air stoichiometric ratio than torrefied pine at 240-75 (see Table 4.3). Therefore, this feedstock (240-30) requires a larger amount of air to reach a given Fr in the gasification process; which leads to increase the nitrogen content in the global reaction. This inert gas is heated by a fraction of the energy released during the gasification resulting in a decrease of the process reaction temperature [19]. Prins et al. [6] also reported an increase in the reaction temperature when torrefied biomass

is used as feedstock in gasification processes. Reaction temperatures for torrefied pine at 210 °C during 30 and 75 minutes are lower than the temperature for 180-120 due to their lower fuel/air stoichiometric ratios by the increase in their carbon contents after torrefaction.

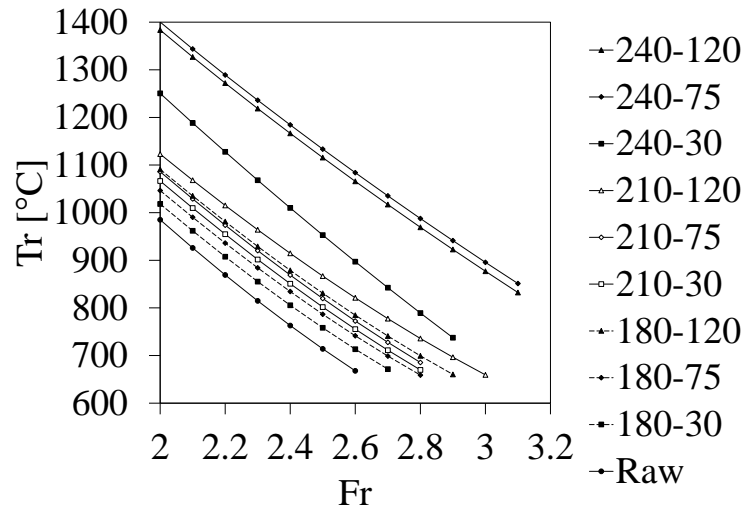


Figure 4.6. Reaction temperature

4.3.3.2. PG composition and heating value

Figure 4.7 shows the PG composition and heating value in function of pretreatment conditions used as feedstock. As mentioned before (section 4.3.2), increasing Fr leads to higher fuel-rich conditions in the gasification process; therefore, a higher amount of gasses with energy content (CO , H_2 , and CH_4) are produced resulting in an increase of the PG heating value. Pérez et al. [19] stated that equilibrium constants of hydrogen reduction with char (Eq. 4.3) and water-gas shift reaction (Eq. 4.4) increase with lower reaction temperature favoring the production of H_2 and CH_4 .

CO concentration tends to increase while H_2 and CH_4 decrease with torrefaction severity due to the reduction in H/C and O/C ratios (see Table 4.3). As expected, torrefied biomass at 240 °C has the highest concentration of CO in the PG. This behavior is related to the high carbon content of these materials. However, despite the difference in PG compositions of the different materials, PG heating value is similar for raw and torrefied pine up to 210-120 (variation of 2% regardless the Fr). Moreover, PG heating value from torrefied pine at 240 °C is higher and decreases slightly regarding torrefaction residence time. Material pretreated at this temperature exhibits higher carbon content and decreases with residence time due to oxidation reactions that occur during the process [15]. Studies about

gasification processes using torrefied biomass reported a similar behavior to the findings of the present work [6], [20]. Furthermore, it has also indicated that gas yield in a gasification process using torrefied biomass as feedstock increases [7], [25].

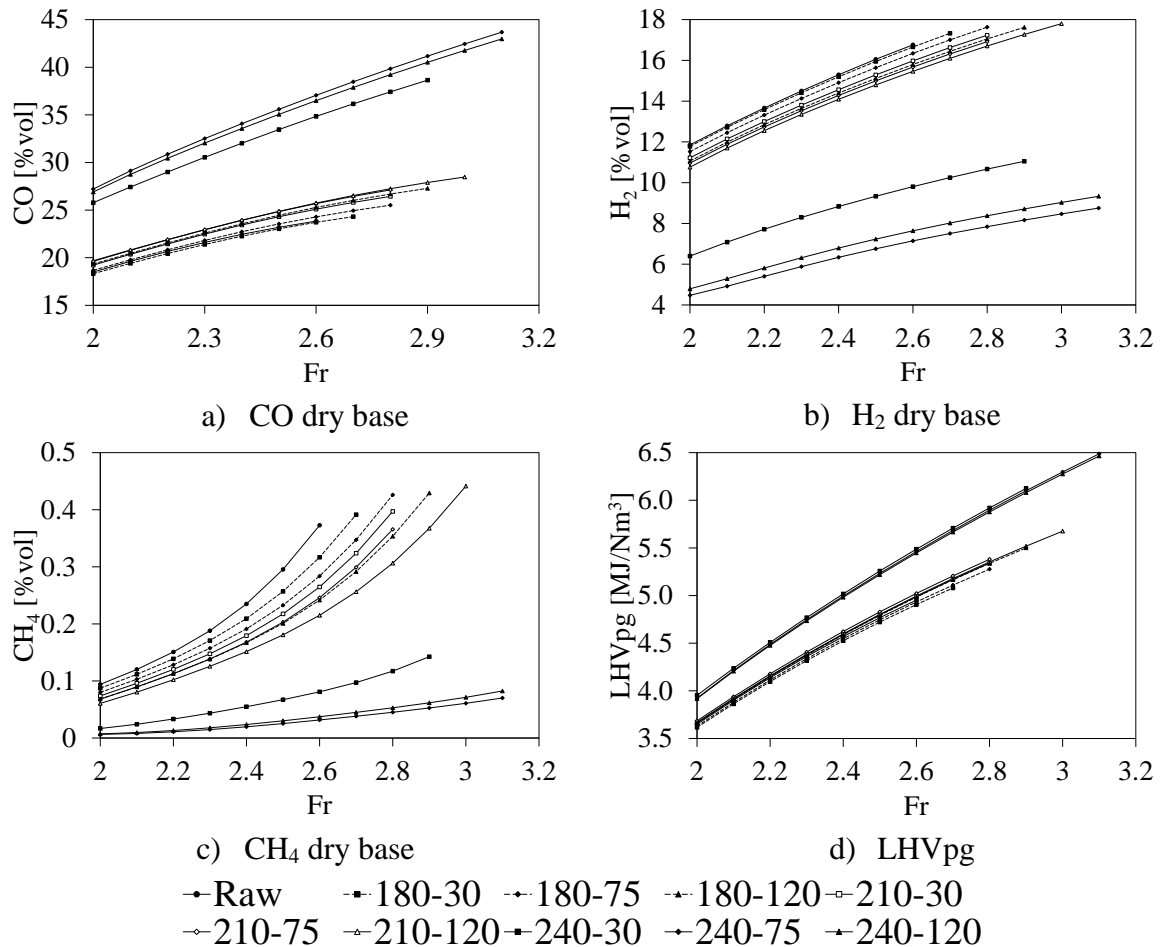


Figure 4.7. PG composition and heating value for raw and torrefied pine wood

4.3.3.3. Cold gas efficiency and engine fuel quality

Figure 4.8 shows the CGE for raw and torrefied pine wood. Increasing Fr results in an increase of CGE for all feedstock studied in the gasification process. As mentioned before (sections 4.3.3.2), gasses with energy content such as CO, CH₄, and H₂ increase their concentrations in the PG with increasing Fr. The combined effect of the concentrations of these gasses on the PG enhances its heating value (Figure 4.7) resulting in the increase of the CGE.

Regarding torrefaction process, CGE tends to decrease with torrefaction severity for a given Fr, except for 240-30. The heating value of the PG tends to increase slightly for torrefied pine up to 210-120 (around 3%). However, the input energy using torrefied

biomass is higher since the changes in its heating value are greater with respect to the raw material (around 5%). Therefore, a lower CGE is reached for torrefied biomass used as feedstock in the gasification process. The CGE for torrefied pine at 240-30 is similar to the CGE of the raw material because this condition reaches the maximum heating value in the PG regardless the Fr of the process (Figure 4.7d). For achieving higher CGE using torrefied biomass, it is necessary to move towards more fuel-rich conditions (i.e. higher Fr) in the gasification process with lower amount of solid byproduct (see section 4.3.2). Kuo et al. [25] reported lower CGE for torrefied biomass at high temperatures (300 °C) due to similarities in the heating value of the PG regarding the raw material.

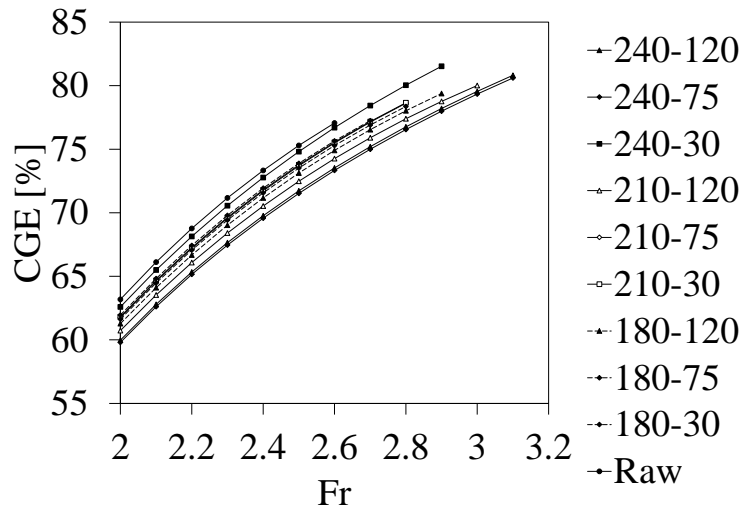


Figure 4.8. CGE for raw and torrefied pine wood

PG from gasification process can be used for heat or power generation in internal combustion engines [1]. Therefore, it is necessary to study its behavior in these applications. The effective power (\dot{N}_e) of an engine is estimated by Eq. 4.8 [39].

$$\dot{N}_e = K_D \cdot K_o \cdot EFQ \quad (4.8)$$

K_D and K_o are parameters that related engine design and operating conditions, respectively. The engine fuel quality (EFQ) relates PG heating value (LHV_{pg}), its fuel/air stoichiometric ratio ($F_{stq,pg}$), and air mole fraction in the PG-air mixture (Y_{air}). This parameter is calculated according to Eq. 4.9 [39].

$$EFQ = LHV_{pg} \cdot Y_{air} \cdot F_{stq,pg} \quad (4.9)$$

For a stationary engine in a power plant, K_D and K_o are constants; therefore, the effective power depends on PG composition and its heating value. Figure 4.9a shows the EFQ for raw and torrefied pine wood in function of Fr. Higher Fr in the gasification process leads to increase the EFQ for all materials; this is due to the higher concentration of gaseous fuel in PG with Fr which increases the PG heating value favoring the EFQ (Eq. 4.9). Likewise, $F_{stq,pg}$ tends to decrease because more air is needed to burn the PG under stoichiometric conditions; hence, air fraction in the mixture also increase with Fr. Therefore, higher air fraction in the mixture and higher PG heating value result in an increase in the energy density of the stoichiometric mixture PG-air; i.e. higher EFQ values [19]. Pérez et al. [19] obtained lower EFQ values for gasification of different Colombian wood species. However, they reported similar trend to the found in this work; i.e. increasing EFQ with Fr. This result shows that torrefaction under an oxidizing atmosphere is suitable to produce gaseous fuels with acceptable quality for internal combustion engine applications.

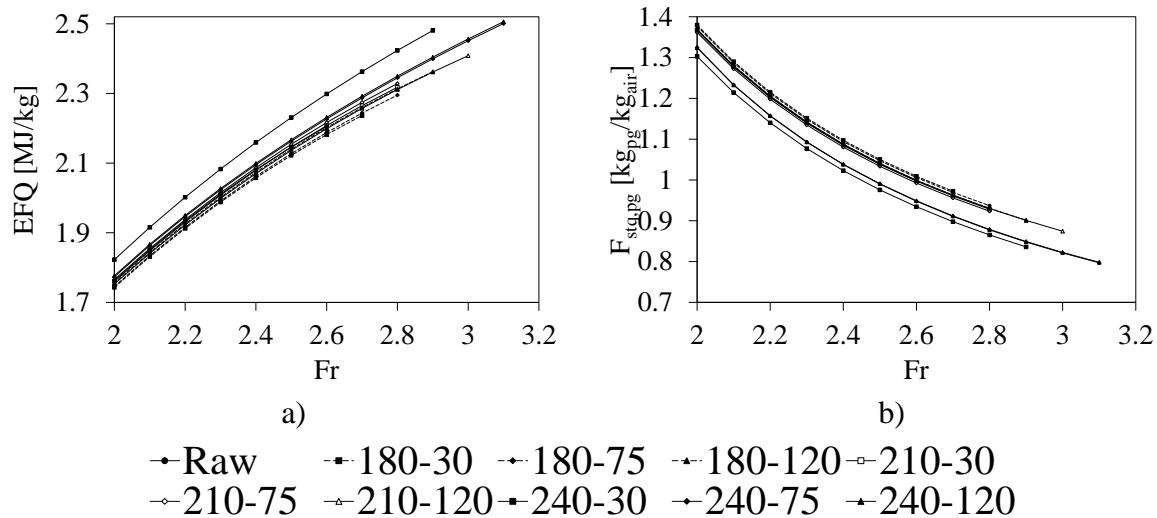


Figure 4.9. EFQ and fuel/air stoichiometric ratio of PG for raw and torrefied pine wood

For a given value of Fr, EFQ is similar for raw and torrefied material, except for 240-30. There is a slight trend to increase with torrefaction severity; i.e. lower O/C ratio. The share of heating value and air fraction in PG-air mixture prevail over the reduction in the fuel/air stoichiometric ratio. The highest EFQ values are reached for a PG from torrefied pine wood at 240-30; this is due to this feedstock has the highest heating value (see Table 4.3). This

result also supports the idea that torrefaction is a suitable process to upgrade biomass properties for gasification processes coupled to internal combustion engines.

Conclusions

Gasification performance of torrefied biomass under an oxidizing atmosphere using a model under thermochemical equilibrium is studied. Model was extended from previous versions to take into account new products from associated with biomass sulfur gasification and the biochar production as a byproduct of the process. Furthermore, the model was validated using experimental data of a gasification process using torrefied biomass. According to validation results, the errors for the different response variables exhibit good agreement between model and the experimental data, especially for heating value of the producer gas and for cold gas efficiency. The global relative error of the model is 8.5%. Therefore, the model in thermochemical equilibrium is a useful tool to study the gasification performance using upgraded biomass by torrefaction as feedstock.

Regarding the gasification process using torrefied biomass under an oxidizing atmosphere, several conclusions can be highlighted under the simulation conditions of the present work. Biochar production has a direct influence on the gasification performance due to it modifies the actual fuel/air equivalence ratio. Higher biochar production conducts to the higher availability of air to react with the biomass; hence, fuel/air ratio tends to combustion conditions reducing the concentration of gasses with energy content such as CO, H₂, and CH₄ and increasing the concentration of others such as CO₂ and H₂O in the PG. The complete combustion of the biomass leads to increasing the reaction temperature of the process. Using torrefied biomass allows to obtaining higher reaction temperatures for a given fuel/air equivalence ratio regarding the raw material. Therefore, higher process efficiencies can be achieved using upgraded biomass as feedstock.

Thermodynamic parameters of the gasification process are enhanced with increasing fuel/air equivalence ratio of the process. Higher equivalence ratios increase the amounts of gasses with energy content (e.g. CO, H₂, and CH₄) in the producer gas; therefore, higher heating value, cold gas efficiency, and EFQ are obtained. Regarding torrefaction conditions, process efficiencies decrease slightly with torrefaction severity; this result is due to PG heating value does not change significantly regarding the raw material. However, there is a trend to increase the heating value with torrefaction severity, especially for the

highest temperature analyzed (240 °C). This behavior allows improving the quality of the PG for internal combustion engine applications. Thereby, torrefaction under an oxidizing atmosphere to upgrade biomass prior its gasification is a suitable process to improve process performance, especially for internal combustion engine applications of the producer gas.

Acknowledgements

The authors acknowledge Universidad de Antioquia for the financial support of this research through Projects “Estrategias de integración de la madera plantada en Colombia en conceptos de biorrefinería termoquímica: Análisis termodinámico y caracterización de bioproductos – PRG 2014-1016” and “Sostenibilidad 2015-2016”, and through the “Estudiante instructor” program.

References

- [1] J. D. Martínez, K. Mahkamov, R. V. Andrade, and E. E. Silva Lora, “Syngas production in downdraft biomass gasifiers and its application using internal combustion engines,” *Renew. Energy*, vol. 38, no. 1, pp. 1–9, 2012.
- [2] M. Puig-Arnavat, J. C. Bruno, and A. Coronas, “Review and analysis of biomass gasification models,” *Renew. Sustain. Energy Rev.*, vol. 14, no. 9, pp. 2841–2851, 2010.
- [3] UNFCCC. Conference of the Parties (COP), “Adoption of the Paris Agreement,” *Paris Clim. Chang. Conf. - Novemb. 2015, COP 21*, vol. 21932, no. December, p. 32, 2015.
- [4] C. Berrueco, J. Recari, B. M. Güell, and G. Del Alamo, “Pressurized gasification of torrefied woody biomass in a lab scale fluidized bed,” *Energy*, vol. 70, pp. 68–78, 2014.
- [5] S. Ramos-Carmona, J. F. Pérez, M. R. Pelaez-Samaniego, R. Barrera, and M. Garcia-Perez, “Effect of torrefaction temperature on properties of Patula Pine,” *Maderas. Cienc. y Tecnol.*, 2017.
- [6] M. J. Prins, K. J. Ptasinski, and F. J. J. G. Janssen, “More efficient biomass gasification via torrefaction,” *Energy*, vol. 31, no. 15, pp. 3458–3470, 2006.
- [7] C. Couhert, S. Salvador, and J. M. Commandré, “Impact of torrefaction on syngas production from wood,” *Fuel*, vol. 88, no. 11, pp. 2286–2290, 2009.

- [8] M. R. Pelaez-Samaniego, V. Yadama, M. Garcia-Perez, E. Lowell, and A. G. McDonald, "Effect of temperature during wood torrefaction on the formation of lignin liquid intermediates," *J. Anal. Appl. Pyrolysis*, vol. 109, pp. 222–233, 2014.
- [9] W. H. Chen and P. C. Kuo, "A study on torrefaction of various biomass materials and its impact on lignocellulosic structure simulated by a thermogravimetry," *Energy*, vol. 35, no. 6, pp. 2580–2586, 2010.
- [10] R. H. H. Ibrahim, L. I. Darvell, J. M. Jones, and A. Williams, "Physicochemical characterisation of torrefied biomass," *J. Anal. Appl. Pyrolysis*, vol. 103, pp. 21–30, 2013.
- [11] V. Repellin, A. Govin, M. Rolland, and R. Guyonnet, "Energy requirement for fine grinding of torrefied wood," *Biomass and Bioenergy*, vol. 34, no. 7, pp. 923–930, 2010.
- [12] K. M. Lu, W. J. Lee, W. H. Chen, S. H. Liu, and T. C. Lin, "Torrefaction and low temperature carbonization of oil palm fiber and eucalyptus in nitrogen and air atmospheres," *Bioresour. Technol.*, vol. 123, pp. 98–105, 2012.
- [13] P. Rousset, L. MacEdo, J. M. Commandré, and A. Moreira, "Biomass torrefaction under different oxygen concentrations and its effect on the composition of the solid by-product," *J. Anal. Appl. Pyrolysis*, vol. 96, pp. 86–91, 2012.
- [14] Y. Uemura, S. Saadon, N. Osman, N. Mansor, and K. Tanoue, "Torrefaction of oil palm kernel shell in the presence of oxygen and carbon dioxide," *Fuel*, vol. 144, pp. 171–179, 2015.
- [15] W. H. Chen, K. M. Lu, W. J. Lee, S. H. Liu, and T. C. Lin, "Non-oxidative and oxidative torrefaction characterization and SEM observations of fibrous and ligneous biomass," *Appl. Energy*, vol. 114, pp. 104–113, 2014.
- [16] W. H. Chen, K. M. Lu, S. H. Liu, C. M. Tsai, W. J. Lee, and T. C. Lin, "Biomass torrefaction characteristics in inert and oxidative atmospheres at various superficial velocities," *Bioresour. Technol.*, vol. 146, no. x, pp. 152–160, 2013.
- [17] J. Li, X. Zhang, H. Pawlak-Kruczek, W. Yang, P. Kruczek, and W. Blasiak, "Process simulation of co-firing torrefied biomass in a 220MWe coal-fired power plant," *Energy Convers. Manag.*, vol. 84, pp. 503–511, 2014.
- [18] C. Ndibe, S. Grathwohl, M. Paneru, J. Maier, and G. Scheffknecht, "Emissions reduction and deposits characteristics during cofiring of high shares of torrefied biomass in a 500kW pulverized coal furnace," *Fuel*, vol. 156, pp. 177–189, 2015.

- [19] J. F. Pérez, A. Melgar, and A. Horrillo, “Thermodynamic methodology to support the selection of feedstocks for decentralised downdraft gasification power plants,” *Int. J. Sustain. Energy*, vol. 6451, no. April, pp. 1–19, 2016.
- [20] Q. Chen, J. S. Zhou, B. J. Liu, Q. F. Mei, and Z. Y. Luo, “Influence of torrefaction pretreatment on biomass gasification technology,” *Chinese Sci. Bull.*, vol. 56, no. 14, pp. 1449–1456, 2011.
- [21] W. H. Chen, C. J. Chen, C. I. Hung, C. H. Shen, and H. W. Hsu, “A comparison of gasification phenomena among raw biomass, torrefied biomass and coal in an entrained-flow reactor,” *Appl. Energy*, vol. 112, pp. 421–430, 2013.
- [22] F. Weiland, M. Nordwaeger, I. Olofsson, H. Wiinikka, and A. Nordin, “Entrained flow gasification of torrefied wood residues,” *Fuel Process. Technol.*, vol. 125, pp. 51–58, 2014.
- [23] G. Xue, M. Kwapinska, A. Horvat, W. Kwapinski, L. P. L. M. Rabou, S. Dooley, K. M. Czajka, and J. J. Leahy, “Gasification of torrefied *Miscanthus × giganteus* in an air-blown bubbling fluidized bed gasifier,” *Bioresour. Technol.*, vol. 159, pp. 397–403, 2014.
- [24] D. Tapasvi, R. S. Kempegowda, K. Tran, Ø. Skreiberg, and M. Grønli, “A simulation study on the torrefied biomass gasification,” *Energy Convers. Manag.*, vol. 90, pp. 446–457, 2015.
- [25] P. C. Kuo, W. Wu, and W. H. Chen, “Gasification performances of raw and torrefied biomass in a downdraft fixed bed gasifier using thermodynamic analysis,” *Fuel*, vol. 117, no. PARTB, pp. 1231–1241, 2014.
- [26] M. Sarkar, A. Kumar, J. S. Tumuluru, K. N. Patil, and D. D. Bellmer, “Gasification performance of switchgrass pretreated with torrefaction and densification,” *Appl. Energy*, vol. 127, pp. 194–201, 2014.
- [27] A. Melgar, J. F. Pérez, H. Laget, and A. Horrillo, “Thermochemical equilibrium modelling of a gasifying process,” *Energy Convers. Manag.*, vol. 48, no. 1, pp. 59–67, 2007.
- [28] R. Álvarez-Rodríguez and C. Clemente-Jul, “Hot gas desulphurisation with dolomite sorbent in coal gasification,” *Fuel*, vol. 87, no. 17–18, pp. 3513–3521, 2008.

- [29] J. D. Martínez, R. Murillo, T. García, and I. Arauzo, “Thermodynamic analysis for syngas production from volatiles released in waste tire pyrolysis,” *Energy Convers. Manag.*, vol. 81, pp. 338–353, 2014.
- [30] J. D. Martínez, E. E. Silva Lora, R. V. Andrade, and R. L. Jaén, “Experimental study on biomass gasification in a double air stage downdraft reactor,” *Biomass and Bioenergy*, vol. 35, no. 8, pp. 3465–3480, 2011.
- [31] Y. A. Lenis, J. F. Pérez, and A. Melgar, “Fixed bed gasification of Jacaranda Copaia wood: Effect of packing factor and oxygen enriched air,” *Ind. Crops Prod.*, vol. 84, pp. 166–175, 2016.
- [32] B. P. Bibens, “Integrating biomass torrefaction pretreatment with gasification: Effect on syngas yield and tar composition,” University of Georgia, 2010.
- [33] A. Friedl, E. Padouvas, H. Rotter, and K. Varmuza, “Prediction of heating values of biomass fuel from elemental composition,” *Anal. Chim. Acta*, vol. 544, no. 1–2, pp. 191–198, 2005.
- [34] Y. Uemura, W. Omar, N. A. Othman, S. Yusup, and T. Tsutsui, “Torrefaction of oil palm EFB in the presence of oxygen,” *Fuel*, vol. 103, pp. 156–160, 2013.
- [35] Y. Bin Yang, C. Ryu, V. N. Sharifi, and J. Swithenbank, “Effect of model and operating parameters on air gasification of char,” *Energy & Fuels*, vol. 20, pp. 1698–1708, 2006.
- [36] C. Di Blasi and C. Branca, “Modeling a stratified downdraft wood gasifier with primary and secondary air entry,” *Fuel*, vol. 104, pp. 847–860, 2013.
- [37] C. Guizani, O. Louisnard, F. J. E. Sanz, and S. Salvador, “Gasification of woody biomass under high heating rate conditions in pure CO₂: Experiments and modelling,” *Biomass and Bioenergy*, vol. 83, pp. 169–182, 2015.
- [38] P. A. Caton, M. A. Carr, S. S. Kim, and M. J. Beautyman, “Energy recovery from waste food by combustion or gasification with the potential for regenerative dehydration: A case study,” *Energy Convers. Manag.*, vol. 51, no. 6, pp. 1157–1169, 2010.
- [39] F. V. Tinaut, A. Melgar, A. Horrillo, and A. D. De La Rosa, “Method for predicting the performance of an internal combustion engine fuelled by producer gas and other low heating value gases,” *Fuel Process. Technol.*, vol. 87, no. 2, pp. 135–142, 2006.

Recommendations for future study

Torrefaction process under an oxidizing atmosphere is a suitable process to upgrade biomass properties for further thermochemical processes such as fixed bed gasification. However, for a better understanding of the phenomena involved in the pretreatment process, the following studies deserves further investigation.

- To evaluate the effect of torrefaction conditions under an oxidizing atmosphere on the devolatilization kinetics in order to study with more detail the changes in reactivity of pretreated material.
- To study the volatiles released during the torrefaction process to determine the effect of oxygen in the carrier gas on its composition.
- To determine the efficiency of the torrefaction process integrated to a further thermochemical process, e.g. gasification to evaluate the technical and economic feasibility of the thermal pretreatment.
- To evaluate the pyrolysis behavior of torrefied biomass to determine the composition and possible application of the producer bio-oil.
- To conduct gasification process experimentally to verify the finding obtained with the model in thermochemical equilibrium. Additionally, to characterize the biochar obtained during the gasification process to find possible applications of the byproduct and give it an added value.

Appendix A. Correlation to estimate the hardgrove grindability index (HGI)

In order to find an equation that aids to predict the grindability behavior (HGI index) of a torrefied biomass, it was calculated a correlation of the HGI in function of the chemical composition of biomass; namely proximate analysis. Experimental data used in the study were the reported by Ibrahim et al. [1], Williams et al. [2], and Ohliger et al. [3]. From these works, 27 experimental HGI, and proximate analysis were obtained for different kinds of biomass (see Table 1). Torrefaction conditions were coded as temperature-residence time; e.g. 200-30 means a torrefaction conditions of 200 °C and 30 minutes.

Table A.1. Experimental data reported in literature

Authors	Species	Torrefaction condition	Proximate analysis [wt.% db ^a]			HGI
			VM	FC	Ash	
Williams et al.	Wood pellets	Raw	82.6	13.3	4.1	18
	Sunflower pellets	Raw	78.5	15.7	5.8	20
	Eucalyptus pellets	Raw	85.2	11.6	3.2	22
	Steam exploded pellets	Raw	78.5	17.3	4.3	29
	Olive cake	Raw	71.4	18.4	10.3	14
Ibrahim et al.	Willow	Raw	84.8	15.2	0.5	32
	Willow	270-30	73.8	26.2	0.5	64.6
	Willow	290-30	63.2	36.8	1.1	86.4
	Eucalyptus	Raw	80.4	19.6	1.6	32
	Eucalyptus	270-30	67.9	32.1	1.6	38.9
	Eucalyptus	270-60	71.2	28.8	2	46.8
	Eucalyptus	290-30	60.3	39.7	2.2	79.7
	Softwood	Raw	83	17	0.1	32
	Softwood	270-30	79.7	20.3	0.1	41.5
	Softwood	270-60	78.3	21.7	0.3	46.4
	Softwood	290-30	71.8	28.2	0.4	69.2
	Hardwood	Raw	83.2	16.9	0.7	32
	Hardwood	270-30	72.2	27.8	1	43.3
Hardwood	270-60	72	28	1.6	41.8	
Hardwood	290-30	64.6	35.4	2.1	63.3	
Ohliger et al.	Beechwood	280-40	71.2	28.07	0.88	50
	Beechwood	270-40	76.43	22.8	0.99	36
	Beechwood	290-40	66.81	32.46	0.92	74

Beechwood	300-40	56.82	42.03	1.49	122
Beechwood	280-20	74.72	24.58	0.9	38
Beechwood	280-60	68.43	30.84	0.95	68
Beechwood	280-40	68.4	30.83	0.96	63
Beechwood	280-40	72.76	26.5	0.85	40

^a dry basis

An analysis of variance (ANOVA) was conducted to establish if volatile matter, fixed carbon, ash, and their interactions have a significant effect on the HGI. Table 2 shows the results of the ANOVA. It can be seen that fixed carbon and its interaction do not have a significant effect on the HGI since this parameter is calculated by the difference in the proximate analysis.

Table A.2. Results of the ANOVA

Source	Sum of squares	Df	Mean square	F-Ratio	p-Value
Ash ²	662.479	1	662.479	20.90	0.0004
VM	7855.67	1	7855.67	247.83	0.0000
FC	44.1417	1	44.1417	1.39	0.2563
Ash	293.858	1	293.858	9.27	0.0082
FC*VM	940.839	1	940.839	29.68	0.0100
MV*Ash	629.741	1	629.741	19.87	0.0005
FC*Ash	24.0812	1	24.0812	0.76	0.3972
Model	10450.8	7			

The correlation to estimate the HGI in function of proximate analysis was determined with a $R^2=0.93$. Volatile matter (VM) and ash contents of biomass are in wt. % on a dry basis.

$$HGI = 1147.05 + 0.149 \cdot VM^2 - 20.775 \cdot VM - 82.213 \cdot ash + 0.931 \cdot MV \cdot ash$$

References

- [1] R. H. H. Ibrahim, L. I. Darvell, J. M. Jones, and A. Williams, "Physicochemical characterisation of torrefied biomass," *J. Anal. Appl. Pyrolysis*, vol. 103, pp. 21–30, 2013.
- [2] O. Williams, C. Eastwick, S. Kingman, D. Giddings, S. Lormor, and E. Lester, "Investigation into the applicability of Bond Work Index (BWI) and Hardgrove Grindability Index (HGI) tests for several biomasses compared to Colombian la Loma coal," *Fuel*, vol. 158, pp. 379–387, 2015.
- [3] A. Ohliger, M. Förster, and R. Kneer, "Torrefaction of beechwood: A parametric study including heat of reaction and grindability," *Fuel*, vol. 104, pp. 607–613, 2013.

Appendix B. Engine fuel quality (EFQ) deduction

According to Tinaut et al. [1], the effective efficiency of an engine is defined by

$$\eta_e = \frac{\dot{N}_e}{\dot{m}_f LHV_{pg}} \quad (\text{B.1})$$

Where \dot{N}_e (kW) is the effective power, \dot{m}_f (kg/s) and LHV_{pg} (kJ/kg) are the mass flow and the heating value of the producer gas. Reordering the equation, the effective power of an engine is

$$\dot{N}_e = \eta_e \dot{m}_f LHV_{pg} \quad (\text{B.2})$$

From the fuel/air equivalence ratio (Fr), the actual mass flow of the producer gas can be estimated as

$$Fr = \frac{F_{act}}{F_{stq}} = \frac{\left(\frac{\dot{m}_f}{\dot{m}_a}\right)_{act}}{\left(\frac{\dot{m}_f}{\dot{m}_a}\right)_{stq}} \quad (\text{B.3})$$

$$\dot{m}_{f,act} = \dot{m}_{a,act} F_{stq} Fr \quad (\text{B.4})$$

Where F_{stq} is the fuel/air stoichiometric ratio ($\text{kg}_{\text{fuel}}/\text{kg}_{\text{air}}$) and $\dot{m}_{a,act}$ (kg/s) is the actual air mass flow in the gasification process. Furthermore, according to Heywood [2], the volumetric efficiency of an engine is

$$\eta_v = \frac{\dot{m}_m}{\dot{m}_{m,ref}} = \frac{\dot{m}_{f,act} + \dot{m}_{a,act}}{V_T \rho_{m,ref} n i} \quad (\text{B.5})$$

Where V_T is the engine displacement (m^3), $\rho_{m,ref}$ is the reference mixture density (kg_m/m^3) for the intake manifold pressure and temperature, n is the number of engine revolutions per second (rev/s), and i is an index that depends on the engine type (1 for 2-stroke engines and 1/2 for 4-stroke). Due to it is very difficult to measure the mixture density, this density is estimated from air density. According to Amagat's law

$$\frac{V_{air}}{V_m} = \frac{N_{air}}{N_m} = Y_{air} \quad (\text{B.6})$$

Where Y_{air} is the air molar fraction (mole_{air}/mole_m), V_{air} and V_m are the partial air volume and mixture volume (m³), respectively. The mixture density is then

$$\rho_{m,ref} = \frac{\dot{m}_m}{\dot{V}_{m,ref}} = \frac{\dot{m}_f + \dot{m}_a}{\dot{V}_{m,ref}} \quad (B.7)$$

Replacing Eq. B.6 into Eq. B.7

$$\rho_{m,ref} = \frac{(\dot{m}_{f,act} + \dot{m}_{a,act})Y_{air}\rho_{air,ref}}{\dot{m}_{a,act}} \quad (B.8)$$

Where $\rho_{air,ref}$ is the reference air density (kg_{air}/m³). Therefore, the volumetric efficiency of the engine is

$$\eta_v = \frac{\dot{m}_{a,act}}{V_T Y_{air} \rho_{a,ref} n i} \quad (B.9)$$

The actual air mass flow is

$$\dot{m}_{a,act} = \eta_v V_T Y_{air} \rho_{a,ref} n i \quad (B.10)$$

The molar air fraction is

$$Y_{air} = \frac{N_{air}}{N_m} = \frac{\dot{m}_a/M_{air}}{\dot{m}_a/M_{air} + \dot{m}_f/M_f} = \frac{1/M_{air}}{1/M_{air} + Fr F_{stq}/M_f} \quad (B.11)$$

Replacing Eqs. B.4 and B.10 into Eq. B.2, the effective power is

$$\dot{N}_e = \eta_e \eta_v V_T Y_{air} \rho_{a,ref} n i F_{stq} Fr LHV_{pg} \quad (12)$$

$$\dot{N}_e = K_O \cdot K_D \cdot EFQ$$

$$K_O = n \rho_{a,ref} Fr$$

$$K_D = \eta_e \eta_v V_T i$$

$$EFQ = Y_{air} F_{stq} LHV_{pg}$$

K_O (kg rev/m³s) and K_D (m³/rev) are parameters that depends on the engine operation and engine design, respectively; and the EFQ (kJ/kg) is the engine fuel quality and depends on producer gas composition.

References

- [1] F. V. Tinaut, A. Melgar, A. Horrillo, and A. D. De La Rosa, "Method for predicting the performance of an internal combustion engine fuelled by producer gas and other low heating value gases," *Fuel Process. Technol.*, vol. 87, no. 2, pp. 135–142, 2006.
- [2] J. B. Heywood, *Internal combustion engine fundamentals*, vol. 930. Mcgraw-hill New York, 1988.